Clinical and Translational Imaging
https://doi.org/10.1007/s40336-022-00502-y

EXPERT REVIEW

In vivo brain MR spectroscopy in gliomas: clinical and pre-clinical chances

Francesco Padelli[1] · Federica Mazzi[1] · Alessandra Erbetta[1] · Luisa Chiapparini[1] · Fabio M. Doniselli[1,2] · Sara Palermo[1,3] · Domenico Aquino[1] · Maria Grazia Bruzzone[1] · Valeria Cuccarini[1]

Received: 1 March 2022 / Accepted: 2 May 2022

Abstract

Purpose Gliomas, the most common primary brain tumours, have recently been re-classified incorporating molecular aspects with important clinical, prognostic, and predictive implications. Concurrently, the reprogramming of metabolism, altering intracellular and extracellular metabolites affecting gene expression, differentiation, and the tumour microenvironment, is increasingly being studied, and alterations in metabolic pathways are becoming hallmarks of cancer. Magnetic resonance spectroscopy (MRS) is a complementary, non-invasive technique capable of quantifying multiple metabolites. The aim of this review focuses on the methodology and analysis techniques in proton MRS (1H MRS), including a brief look at X-nuclei MRS, and on its perspectives for diagnostic and prognostic biomarkers in gliomas in both clinical practice and preclinical research.

Methods PubMed literature research was performed cross-linking the following key words: glioma, MRS, brain, in-vivo, human, animal model, clinical, pre-clinical, techniques, sequences, 1H, X-nuclei, Artificial Intelligence (AI), hyperpolarization.

Results We selected clinical works (n = 51), preclinical studies (n = 35) and AI MRS application papers (n = 15) published within the last two decades. The methodological papers (n = 62) were taken into account since the technique first description.

Conclusions Given the development of treatments targeting specific cancer metabolic pathways, MRS could play a key role in allowing non-invasive assessment for patient diagnosis and stratification, predicting and monitoring treatment responses and prognosis. The characterization of gliomas through MRS will benefit of a wide synergy among scientists and clinicians of different specialties within the context of new translational competences. Head coils, MRI hardware and post-processing analysis progress, advances in research, experts' consensus recommendations and specific professionalizing programs will make the technique increasingly trustworthy, responsive, accessible.

Keywords Glioma · Brain MR spectroscopy · In vivo · Clinical · Pre-clinical

Francesco Padelli and Federica Mazzi contributed equally to this work.

✉ Domenico Aquino
domenico.aquino@istituto-besta.it

Francesco Padelli
francesco.padelli@istituto-besta.it

Federica Mazzi
federica.mazzi@istituto-besta.it

Alessandra Erbetta
alessandra.erbetta@istituto-besta.it

Luisa Chiapparini
luisa.chiapparini@istituto-besta.it

Fabio M. Doniselli
fabio.doniselli@istituto-besta.it

Sara Palermo
sara.palermo@istituto-besta.it

Maria Grazia Bruzzone
maria.bruzzone@istituto-besta.it

Valeria Cuccarini
valeria.cuccarini@istituto-besta.it

[1] Neuroradiology Unit, Fondazione IRCCS Istituto Neurologico Carlo Besta, Via Celoria 11, 20133 Milan, Italy

[2] Department of Biomedical Sciences for Health, University of Milan, Milan, Italy

[3] Department of Psychology, University of Turin, Turin, Italy

Published online: 31 May 2022

Abbreviations

2HG	2-HydroxyGlutarate
α-KG	α-KetoGlutarate
AI	Artificial Intelligence
ANN	Artificial Neural Network
BHB	Beta-HydroxyButyrate
CA	Contrast Agent
CHESS	Chemical Shift Selective Saturation
Cho	Choline-containing compounds
CNR	Contrast-to-Noise Ratio
COSY	Correlation Spectroscopy
Cr	Creatine
CSI	Chemical Shift Imaging
d-DNP	Dissolution Dynamic Nuclear Polarization
EGFR	Epidermal Growth Factor Receptor
EPSI	Echo-Planar Spectroscopic Imaging
FID	Free Induction Decay
FLAIR	Fluid-Attenuated Inversion Recovery
GABA	Gamma-AminoButyric Acid
GBM	GlioBlastoma Multiforme
GLAST	GLutamate-ASpartate Transporter
Gln	Glutamine
Glu	Glutamate
Gly	Glycine
GPC	GlyceroPhosphoCholine
GRAPPA	Generalized Autocalibrating Partially Parallel Acquisition
GSH	Glutathione
HP	HyperPolarization
IDH	Isocitrate DeHydrogenases
Lac	Lactate
Lip	Lipids
LASER	Localization by Adiabatic Selective Refocusing
LOH	Loss Of Heterozygosis
MEGA	MEshcher-GArwood
MGMT	O6-Methylguanine-DNA Methyltransferase
mIns	Myo-Inositol
MOIST	Multiple Optimizations Insensitive Suppression Train
MRI	Magnetic Resonance Imaging
MRS	Magnetic Resonance Spectroscopy
^{1}H MRS	Proton Magnetic Resonance Spectroscopy
MRSI	Magnetic Resonance Spectroscopic Imaging-
	mTOR = Mammalian Target Of Rapamycin
NAA	N-AcetylAsparate
ODG	Oligodendroglioma
OVS	Outer Volume Suppression
PC	PhosphoCholine
PCr	PhosphoCreatine
PHIP	ParaHydrogen Induced Polarization
PI3K	PhosphoInositide-3-Kinase
PKC	Protein Kinase C
PRESS	Point REsolved Spectroscopy
RF	RadioFrequency
SABRE	Signal Amplification by Reversible Exchange
SAHA	SuberoylAnilide Hydroxamic Acid
SAR	Specific Absorption Rate
SENSE	Sensitivity Encoding
SLAM	Spectroscopy with Linear Algebraic Modelling
SLIM	Spectral Localization by Imaging
SMS	Simultaneous Multislice Imaging
SNR	Signal-to-Noise Ratio
SPECIAL	SPin ECho Full-Intensity-Acquired Localization
SPICE	Spectroscopic Imaging by Exploiting spatio-spectral Correlation
SSFP	Steady-State Free Precession
STEAM	STimulated Echo Acquisition Mode
SVM	Support Vector Machine
SWAMP	Suppression of Water with Adiabatic-Modulated Pulses
Tau	Taurine
TE	Echo Time
TR	Repetition Time
TERT	TElomerase Reverse Transcriptase
VAPOR	VAriable Power radio-frequency pulses with Optimized Relaxation delays
WET	Water Suppression Enhanced through T1 effects

Introduction

Gliomas are the most common primary brain tumours often associated with dismal prognosis. They have recently been re-classified [1] based not only on histological findings but also on molecular aspects with important clinical implications for prognosis and treatment. As a result, the choice of optimal treatment and management of clinical trials would be enhanced, enabling the analysis of known and novel therapies [1, 2].

Moreover, the metabolic reprogramming in response to oncogenic mutations plays a critical role in tumorigenesis deeply altering intracellular and extracellular metabolites, and affecting gene expression, differentiation and tumour microenvironment [3]. Consequently, alterations in metabolic pathways are important hallmarks of cancer.

Although conventional magnetic resonance imaging (MRI) is the gold standard in gliomas diagnosis and follow-up, it cannot provide information about tumour viability or activity: this can hinder the distinction of treatment effects from tumour progression. The need for accurate in vivo

biomarkers of gliomas metabolic activity represents one of the main research and clinical challenges [4].

Advanced MRI techniques can provide a valuable aid to conventional MRI for a more exhaustive characterization of tumoral tissue, such as the degree of cellularity (diffusion-weighted imaging) and the neo-angiogenesis (perfusion-weighted imaging).

Magnetic resonance spectroscopy (MRS) is a complementary, non-invasive technique capable of quantifying multiple metabolites, thus helping to answer many important clinical questions: differentiating tumours from other focal lesions, identifying the optimal biopsy sites in heterogeneous gliomas as well as improving the in vivo characterization of brain tumours even when surgery is not indicated, monitoring treatment response, and guiding treatment planning [5, 6].

Considering the development of treatments targeting cancer metabolism in clinical trials [7], MRS may play a key role in allowing tissue characterization with a non-invasive metabolic assessment for patients' stratification, monitoring treatment response, prediction and prognosis.

Since almost all biological molecules contain protons and the proton has a high gyromagnetic ratio, proton magnetic resonance spectroscopy (^{1}H MRS) is extensively used to monitor the levels of cellular metabolites, including in the field of neuro-oncology [8].

This review focuses on the methodology and analysis techniques in ^{1}H MRS, including a brief look at X-nuclei MRS, and its perspectives for diagnostic and prognostic biomarkers in gliomas in both clinical practice and preclinical research.

Acquisition

As the metabolism of the brain vary with pathology, MRS can provide invaluable information about a lesion and its peri-lesional environment that is not otherwise available from MRI [9]. While single-voxel spectroscopy results in a high signal from a specific localized brain region, multivoxel spectroscopy (named MR spectroscopic imaging, MRSI, or chemical shift imaging, CSI) covers a larger brain area and can gain different data from heterogeneous tumours and

Table 1 Brief summary of benefits and drawbacks of the main MRS / MRSI pulse sequences used in clinical practice and pre-clinical research

	Method	Benefits	Drawbacks
PRESS	Spin echo MRS	Full signal (spin echo)	Small voxel size
		3D voxel localization	Long acquisition time
		Long minimum TE	
STEAM	Stimulated echo MRS	Sharply defined voxel	Low SNR (stimulated echo)
		Short minimum TE	
		Low RF power, thus low SAR	
LASER	Adiabatic pulses MRS	Absence of chemical shift artifacts	High RF power, thus high SAR
		Long minimum TE	
		Low dependence on B1	
SPECIAL	High signal intensity with short TE	Full signal (as PRESS)	At least two scans required
		Short achievable TE (as STEAM)	Subject motion artifacts
		Low dependence on B1	Long acquisition time
EPSI	Fast CSI with echo planar encoding	High acceleration for larger volumes	Gradients demanding
		Constant *k*-space weighting	Sensible to field inhomogeneity
			Low SNR
			Limited spectral bandwidth
			Limited spatial resolution
2D COSY	2D correlation spectroscopy	Resolves overlapping multiplets of J-coupled spin systems	Residual unsuppressed water contaminations
			Long acquisition time
MEGA-PRESS	MEGA-suppressed MRS	Suppression of overlying metabolites signals	Sensible to field inhomogeneity
		Efficient water suppression	Long acquisition time
		Insensibility to flip angle errors	
		Absence of phase distortions	
		Short minimum TE	

peri-tumoral tissue. The voxel size has to be large enough to obtain a high signal-to-noise ratio (SNR) but at the same time fairly small to provide an adequate spatial resolution. Many efforts have been undertaken in recent years to enhance the acquisition techniques related to spatial resolution, timing, spectral quality, and the role of ^{1}H MRS has advanced from identifying generic glial tumour signatures to the identification of specific onco-metabolites [10].

In the next section, the main MRS acquisition techniques will be discussed. (Table 1) summarizes the benefits and the drawbacks of the reported MRS pulse sequences used in clinical practice and pre-clinical research.

PRESS

The Point RESolved Spectroscopy (PRESS) sequence is the firstly proposed and the most widely used sequence for MRS acquisitions [11]. It is a double spin-echo pulse sequence characterized by three subsequent slice-selective radiofrequency (RF) pulses (90° – 180° – 180°) applied simultaneously to three orthogonal field gradients for shaping the acquisition voxel. Thus, at time TE (echo time) the signal is a spin echo derived only from protons located where the three RF-induced planes overlap and are subjected to all RF pulses.

STEAM

As opposed to PRESS which relies on spin-echo signals, STimulated Echo Acquisition Mode (STEAM) sequence is based on the application of three slice-selective 90° RF pulses to generate a stimulated echo [12]. Compared to PRESS, the STEAM sequence has many advantages. First of all, the minimum reachable TE can be very short allowing short-T2 metabolites detection. Then, the use of only 90° pulses allows for better voxel definition, higher pulse bandwidth thus reducing chemical shift displacement artifacts, and lower applied RF power, i.e., lower SAR (Specific Absorption Rate) levels. Despite this, STEAM is less commonly used than PRESS, primarily because it has a lower SNR than the latter, due to the presence of stimulated echoes instead of spin echoes. Indeed, the PRESS sequence is characterized by a signal doubled with respect to STEAM [13].

LASER

The Localization by Adiabatic Selective Refocusing (LASER) sequence uses a non-slice-selective adiabatic half-passage excitation pulse, before three pairs of adiabatic full-passage refocusing pulses [14, 15]. This technique allows overcome some in vivo MRS limitations [16], in particular additional J-refocused artefactual peaks, chemical shift artifacts and sensitivity to RF field inhomogeneity.

LASER requires long TE values because of the above-mentioned three pairs of adiabatic 180° pulses. In the semi-LASER sequence, one 180° pulse pair is replaced by a slice-selective excitation pulse. This enables the reduction of TE values up to 50 – 30 ms [17–19].

LASER is usually combined with Outer Volume Suppression (OVS) before the localization sequence and VAPOR (VAriable Power radio-frequency pulses with Optimized Relaxation delays) scheme for the water suppression (see the Water suppression paragraph).

SPECIAL

The SPin ECho Full-Intensity-Acquired Localization (SPECIAL) sequence brings together the full signal intensity of PRESS and the short TE of STEAM. SPECIAL uses an alternating slice-selective adiabatic inversion pulse followed by a 90°–180° slice-selective spin-echo sequence [14, 20]. Similarly to LASER, the SPECIAL protocol exploits OVS and VAPOR. SPECIAL method has many advantages, such as the short TE comparable with STEAM, the preservation of the full magnetization, and the reduction of the RF dependence thanks to the adiabatic inversion pulse. Its most significant drawback is that this technique requires at least two acquisitions as the localization is obtained through the subtraction of two subsequent Free Induction Decay (FID) signals, thus making the scan very sensible to subject motion [16].

2D e 3D multivoxel CSI

Spectroscopic maps from multivoxel acquisitions are particularly useful to monitor metabolites' distribution and concentration. The basic sequence in 2D CSI is a PRESS with phase encoding gradients applied in two directions to obtain a planar matrix of acquisition voxels [21]. An example of a 3D CSI sequence is composed of a RF non-selective pulse with phase-encoding gradients in three directions. The major advantages of the multivoxel CSI technique are the coverage of a larger area and a higher spatial resolution compared to single voxel acquisitions. The main disadvantages are the long acquisition times, a lower SNR and an increased possibility of spectral contamination from neighbouring voxels [22, 23].

EPSI

Proton echo planar spectroscopic imaging (EPSI) is a fast MRS technique that exploits the echo-planar encoding with the use of very short TE. It is increasingly used in brain studies thanks to its ability to cover large volumes in a short time while achieving high spatial and temporal resolutions [24].

An oscillating read-out gradient is used to collect a single k-space raw at succeeding time points, allowing simultaneous acquisition of spectral information and spatial localization. Phase-encoding gradients along the other axes permit 2D or 3D acquisitions [25]. EPSI has been employed to map metabolite spatial distributions directly relating them to the brain anatomy [26].

Spiral CSI

Spiral CSI is a fast technique for accelerating the acquisition compared to the traditional phase-encoded CSI. Spiral encoding is an alternative to EPSI obtained by sampling data using oscillating gradients along two axes. Therefore, *k*-space is repeatedly sampled along a curved trajectory from the centre to the periphery. A significant advantage of spiral CSI over EPSI is that it reduces phase errors thanks to the continuous sampling of the k-space centre [27, 28].

Spiral CSI is the ideal technique for hyperpolarized ^{13}C studies. In addition, it has an increasing importance in ^{1}H MRSI of the brain, with a recent strong clinical use for brain tumours [29–31].

2D COSY

Two-dimensional COrrelation SpectroscopY (2D COSY) is a method to separate signals that would overlap in conventional 1D spectroscopy. The resulting data are collected for each voxel in a bi-dimensional plane with two frequency axes (in contrast to the classic chemical shift-intensity graph), thus peak positions are specified by two frequency coordinates [32]. It consists of a 90° RF pulse followed by an additional 90° pulse after an appropriate evolution time. This technique is very useful when multiplets overlap or when many couplings complicate the spectrum analysis [33]. In this sequence, unpaired nuclei are located on the diagonal of the spectral plane, while off-diagonal peaks are generated by coupled nuclei (peaks area is proportional to the number of nuclei contributing to that position). Since 2D COSY is characterized by very long scanning times, EP-COSI (Echo Planar Correlated Spectroscopic Imaging) and ME-COSI (Multi Echo Correlated Spectroscopic Imaging), were adapted, reducing the scanning time to about 20 min [34]. COSY is part of the technical set used for the 2-HydroxyGlutarate (2HG) detection in Isocitrate DeHydrogenases (IDH)-mutated gliomas [35].

MEGA

MEshcher-GArwood (MEGA) is a frequency selective method [36] proposed for achieving solvent suppression in MR pulse sequences based on either spin echo or stimulated echo acquisition.

MEGA water suppression is based on the application of two frequency selective 180° refocusing pulses. This technique has some advantages, including the insensitivity to flip angle errors, the absence of resulting phase distortion and the easiness of implementation since the RF pulses are identical [37]. It is widely used both with PRESS and STEAM sequences.

MEGA-PRESS was introduced to exploit the MEGA suppression scheme for PRESS sequences. It has been used for Gamma-AminoButyric Acid (GABA) measurements since other techniques can hardly detect this neurotransmitter peaks, due to the overlap with other metabolites [38]. Another application of MEGA-PRESS and of tailored PRESS sequences is the quantification of 2HG to determine the IDH status of brain gliomas [39].

Water suppression

MRS exploits the principle that protons belonging to different compounds resonate at slightly different Larmor frequencies (chemical shift).

Water is the major component of brain tissues. Since its concentration is in the molar range,

water protons signal overcomes the ones generated by small metabolites that are present in millimolar concentrations. Thus, methods aimed to suppress the water in vivo prominent signal at ~ 4.68 ppm are mandatory.

A commonly used approach is the CHESS (Chemical Shift Selective Saturation) [40]. Typical CHESS variants that allow an improved water suppression, despite requiring a longer acquisition time, are MOIST (Multiple Optimizations Insensitive Suppression Train), SWAMP (Suppression of Water with Adiabatic- Modulated Pulses), VAPOR (VAriable Power radio-frequency pulses with Optimized Relaxation delays), and WET (Water Suppression Enhanced through T1 effects) [41–44]. Frequency-selective suppression pulses can be executed preliminary or in the middle of the spectroscopic acquisition: for example, while STEAM sequence performs CHESS-like saturation during the mixing time, MEGA is included between 180° pulses [36].

Acceleration methods

In vivo MRSI long acquisition times are due to the slow phase-encoding gradients needed to properly encode chemical shift and to the long time required by multivoxel localization [45]. Acquisition time reduction can be reached by decreasing the pulse sequence Repetition Time (TR) or acquiring multiple echoes in a single TR.

SSFP (Steady-state free precession) is a gradient-echo pulse sequence in which the residual transverse magnetization is maintained between successive excitation cycles. To reach a steady state, the magnetization must have the same

behaviour in every TR. The k-space is sampled point by point with very short TR values [46]. A low spectral resolution was reachable by means of the original SSFP scheme used in first preclinical studies analysing only single metabolites at a time [47]. Later, when acquisition was improved to attain higher spatial and spectral resolution, research on the human brain began [48].

The turbo-spin echo technique encodes multiple *k*-space lines in a single TR. Unlike conventional spin-echo sequences, multiple 180° pulses with different phase-encoding gradients are used after the initial 90° pulse. Scan times can be reduced from 30 to about 10 min [49], but the use of this method is limited by the loss in SNR and spectral resolution, the increased sensitivity to lipid contamination and the significant T2-decay with the consequent decrease in low-T2 metabolites signal [24, 25, 45].

K-space under-sampling is another method suitable for accelerating both MRI and MRSI sequences. Since a smaller subset of k-space data is acquired, the reconstruction of the missing points is mandatory. GRAPPA (Generalized Autocalibrating Partially Parallel Acquisition) and SENSE (Sensitivity Encoding) are the most widely used parallel imaging acquisition schemes, with scan times reduced from 30 to 6–10 min [50, 51]. SMS (Simultaneous Multislice Imaging) technique exploits the simultaneous excitation of multiple slices with a single RF pulse [52]. The Compressed Sensing MRI exploits the intrinsic sparsity of medical images to undersample *k*-space and it allows to lower the acquisition time from 15 to about 3 min [25, 53].

To improve the quality of the results obtained with accelerated MRSI techniques, spatial and spectral a priori information can be incorporated in data reconstruction. In SLIM (Spectral Localization by Imaging), the acquisition voxel can be shaped to the arbitrary shape of brain structures or lesions, but with the restrictive hypothesis of compartmental metabolic homogeneity [54]. SLAM (Spectroscopy with Linear Algebraic Modelling) replaces the SLIM compartmental homogeneity with a set of voxels characterized by the same metabolite concentrations [55]. SPICE (Spectroscopic Imaging by Exploiting spatio-spectral Correlation) exploits both spectral and spatial a-priori knowledge so that the spectrum of each voxel is represented by the linear superposition of a small number of basis functions relative to specific subspaces (including metabolites, lipids, water and macromolecules) [45, 56, 57].

Post-processing: metabolite's quantification

MRS aims to analyse the chemical composition of tissues to detect even millimolar concentrations of metabolites that would indicate a particular pathological condition. The most investigated metabolites by ^{1}H MRS in neuro-oncology are N-AcetylAsparate (NAA), choline-containing compounds (Cho) including phosphocholine (PC), glycerophosphocholine (GPC), and free choline, GABA, lactate (Lac), free lipids (Lip), creatine (Cr), phosphocreatine (PCr), glutamate (Glu) and glutamine (Gln) also referred as the composite Glx peak, myo-Inositol (mIns), glycine (Gly), glutathione (GSH), taurine (Tau), Beta-HydroxyButyrate (BHB) and more recently 2HG [8, 58]. The area under the peak is proportional to the concentration of the metabolite(s) responsible for generating that signal [59]. The acquired spectra will then be fitted to perform an absolute quantification or to calculate the signal ratios between metabolites peaks. Peak integration and other techniques can be performed after water signal suppression.

Peak integration (traditional approach)

The easiest method to quantify peaks amplitude consists in calculating the area under the peak in the frequency domain [60–62] using simple numerical integration. The first step is to define the frequency range where the peak of interest falls. The area under the curve is then calculated and an estimate of the baseline is subtracted. When dealing with clearly distinguishable signals, this simple approach works well.

Peak fitting methods and a-priori knowledge approach

For in vivo studies, the utmost complexity of spectroscopic data requires algorithms for fitting peaks to a mathematically defined model with a known integral value, which are far more accurate in estimating metabolic concentrations to solve the problem of overlapping peaks. These methods are more useful if combined with a priori information about the metabolites set giving rise to the spectrum [63]. The most widely used software solutions based on these approaches are JMRUI (Java-based Magnetic Resonance User Interface), LCModel (Linear Combination Model) and INSPECTOR.

JMRUI is a free software that employs a Java-based graphical user interface to perform advanced time-domain analysis on MRSI data. It includes two major types of quantification methods, black-box and interactive methods, such as AMARES (Advanced Method for Accurate, Robust and Efficient Spectral fitting) using a priori knowledge and QUEST, based on the availability of metabolites signal basis set [63, 64].

Recently, LCModel became a free software and it is capable of performing frequency domain analyses of MRS data, requiring little user inputs [65]. It benefits from the maximum possible level of a-priori knowledge (e.g., information on the position and intensity of metabolite peaks) through a predetermined series of basis sets. Magnetic field strength and pulse sequence TE determine loaded basis functions.

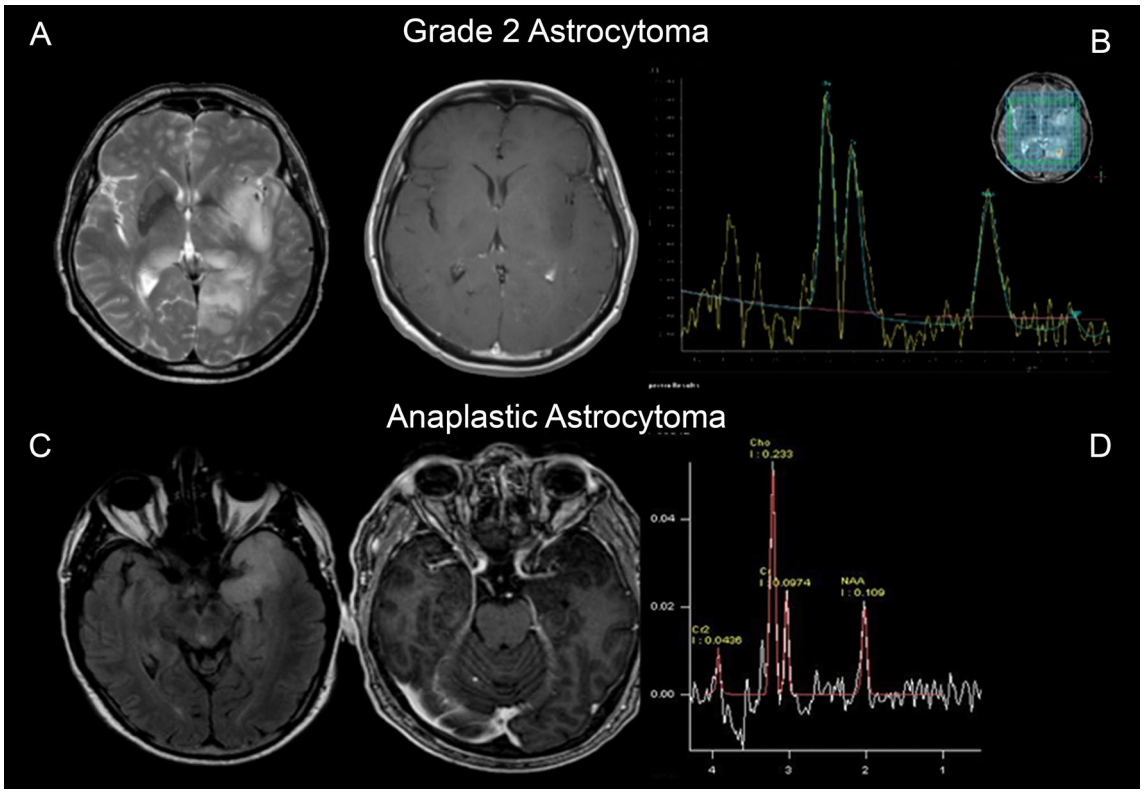

Fig. 1 **A**, **C** left to right: diffuse brain gliomas, hyperintense on long TR (T2/FLAIR) sequences, without contrast enhancement (T1-weighted post-Gadolinium MRI); **B** MRSI shows slight elevation in Cho/Cr ratio and reduced NAA in grade 2 Astrocytoma; **D** pronounced Cho/Cr increase and NAA decrease in grade 3 Astrocytoma

Results of the analysis pipeline include, along with the table of metabolites concentrations with their standard deviations, a graphical depiction of the acquired spectrum in the frequency domain.

MRS data can be easily converted to concentrations of metabolites also using INSPECTOR, which is a free and intuitive software application. It is developed in MATLAB (https://it.mathworks.com/products/matlab.html) and it is managed through a graphical interface. As with LCModel, metabolites quantification is performed by fitting acquired data based on a linear combination of spectra models [66].

MRS for glioma characterization in clinical practice

From a technical point of view, the echo time (TE) used in ^{1}H MRS acquisitions defines which metabolites can be detected and quantified, depending on their T2 relaxation time besides the peaks overlapping and the tissue concentration.

"Long-T2 metabolites"

The expression "long-T2 metabolites" refers to a metabolite set that can be revealed by long TE (in the order of 140 ms) pulse sequences and include Cho, Cr, NAA, Lac and Lip [58].

NAA gives the largest signal in the healthy brain, it is synthesized in neurons, and it is considered a neuronal marker and thus a neuronal health, functionality, and density indicator. The Cho signal comes from the precursors and breakdown products of the membrane phospholipid phosphatidylcholine; thus, Cho peak intensity is associated with cell proliferation. High levels of Cho together with reduced levels of NAA can discriminate between regions of tumour and normal brain [67] while a decrease in the peak of NAA is a hallmark of lower-grade gliomas even in the absence of Cho increase [68]. A different arrangement of these metabolites can help determine whether the tumour has infiltrated beyond the enhanced lesion, which in turn can guide the selection for biopsy and for radiotherapy [69] (Fig. 1).

High-grade gliomas may be misdiagnosed as low-grade gliomas by conventional MRI and some studies reported that MRSI can detect early shifts to anaplasia sooner than other MRI techniques [70]. In studies mostly focusing on

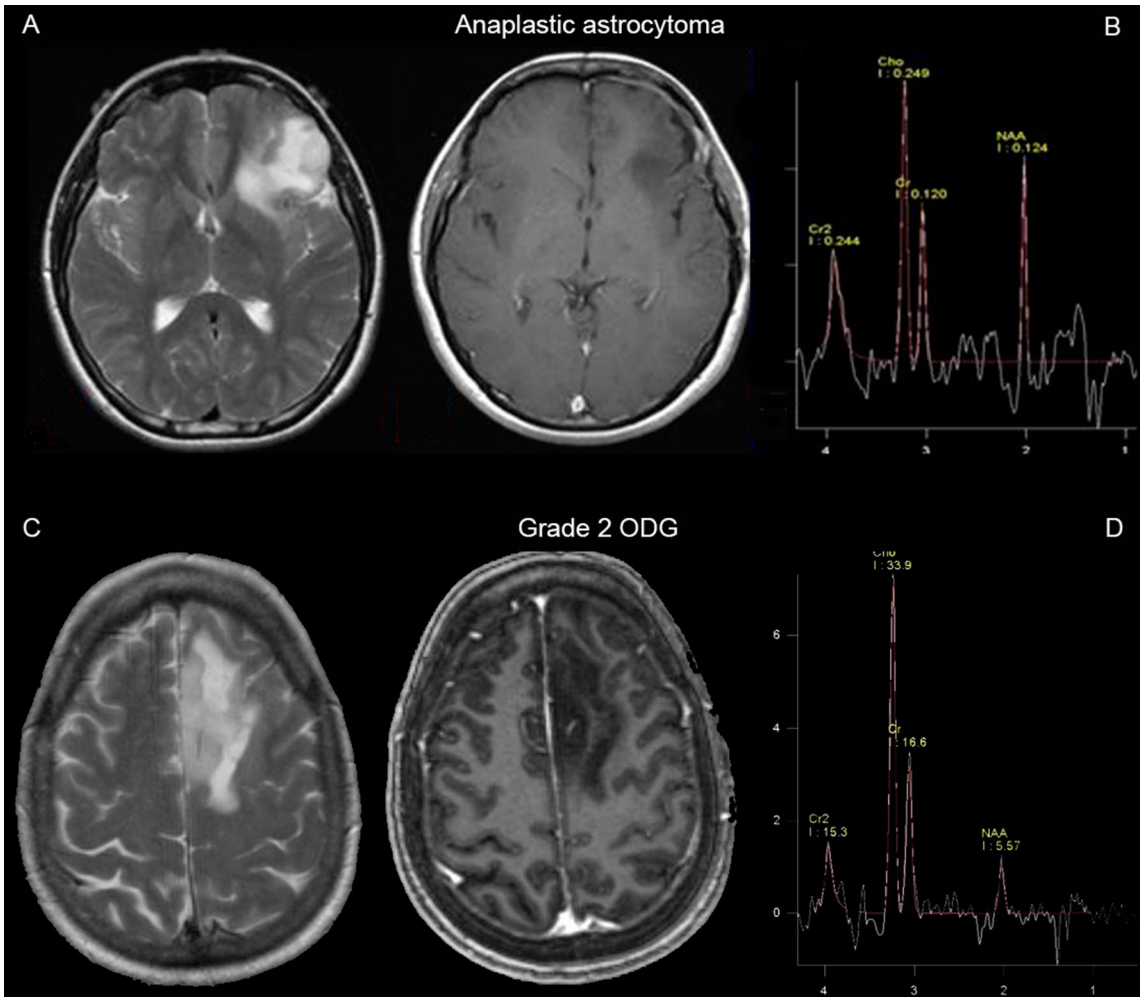

Fig. 2 **A**, **C** left to right: frontal cortical-subcortical brain gliomas, hyperintense on T2-weighted MRI, without contrast enhancement (T1-weighted post-Gadolinium MRI); **B** MRSI shows elevation in Cho/Cr ratio, a noticeable Lac peak, and reduced NAA in grade 3 Astrocytoma; **D** even more pronounced Cho/Cr increase, a noticeable Lac peak, and NAA decrease in grade 2 ODG

low-grade glioma and glioblastoma multiforme (GBM), Cho/NAA and Cho/Cr ratios as well as the presence of Lac or Lip have been identified as useful parameters in determining the glioma grade and in predicting survival [69, 71, 72]. Nevertheless, in cohorts that included only gliomas without enhancement and with scarce perilesional oedema [73], the Cho/Cr values were similar in grades II and III and slightly higher in grade IV.

Generally, the diagnostic accuracy of the Cho/Cr ratio was slightly higher compared to Cho/NAA or NAA/Cr ratios [73]. The difference between tumour and normal parenchyma was quantified by a z-score metric to help accurately describe metabolic lesions. This index was named Cho to NAA Index (CNI) and it resulted to be more robust than metabolites ratios and absolute quantification [74].

Lip and Lac [75, 76] are substantially absent in the normal brain, and they indicate areas of cell death and necrosis (as in grade IV gliomas or radiation necrosis) or hypoxia (as in aggressive gliomas or antiangiogenic therapy) [58, 77] (Fig. 2), respectively.

The quantification of these peaks requires a magnetic field strength ≥ 1.5 T for spectral resolution.

"Short-T2 metabolites"

The "short-T2" (sequence TE below 50 ms) metabolic set includes mIns, Gly, Glu, Gln and GSH [58]. mIns is an osmolyte present in astrocytes and linked to the cell membrane and myeline, whose role as PKC (protein kinase C) activation promoter may be associated with aggressive behaviour of high-grade gliomas [78]. The mIns and Gly peaks often overlap. Increased mIns/Cr, [mIns + Gly]/Cr and Gly/Cr ratios were found in all grades of glial tumours compared with normal-appearing white matter [79]. In vivo and *ex* vivo MRS studies suggested mIns/Cho ratio

may help differentiate between low-grade and high-grade gliomas, as well as gliosis from recurrent glioma [80].

The Gln pathway is emerging as a marker of cancer prognosis and a target for new treatments. Gliomas are characterized by an abnormal consumption of Gln as an energy source, thus increased Gln concentrations may be associated with treatment resistance and proliferation.

In murine models and in preliminary data about glioma patients, Glu has been detected in enhancing lesions and at higher levels in perifocal FLAIR (FLuid-Attenuated Inversion Recovery) hyper-intensities as to trace the infiltrating path [81].

The quantification of these peaks is better recognized at high field strength (≥ 3 T) for higher spectral resolution.

Assessment of glioma type

Gliomas are diagnosed and classified on the basis of the combination between histology and molecular markers [1]. Specifically, IDH1/2 mutations, 1p/19q loss of heterozygosis (LOH), histone H3 alteration, epidermal growth factor receptor (EGFR), 10q deletion, telomerase reverse transcriptase (TERT) and ATRX mutation, and O-6-methylguanine-DNA methyltransferase (MGMT) methylation are useful pathology indicators.

Low-grade gliomas represent 30% of all gliomas [82], their evolution is towards malignancy although the survival rates range from less than 2 years in IDH wild-type GBM to more than 10 years in IDH mutant-1p19q LOH oligodendroglioma (ODG). Clinical approaches range from ‘‘wait and see’’ to early diagnosis through biopsy or surgical resection [83].

An increase in Cho/NAA and Cho/Cr reflects a trend of malignancy, with the exception of ODG (Fig. 2), considered less aggressive due to their peculiar structure [71, 84]. The Gln and Glu levels have been described to be increased in low-grade ODG compared with low-grade astrocytomas [85] and mIn/Cr might help distinguish ODG and astrocytomas [86].

The loss of two enzymes on chromosome 1p leads to cystathionine accumulation and MRS cystathionine levels were found higher in 1p19q LOH. Upon verification of its diagnostic validity, cystathionine could be a biological marker for ODG [87].

IDH status and 2HG-MRS

IDH1 (97%) and IDH2 gene mutations are reported in about 86% of grade II and III gliomas while in secondary GBM are initial and stable mutations. IDH1 is the cytosolic enzyme that catalyses the oxidative decarboxylation of isocitrate to α-KetoGlutarate (α-KG) and IDH1-mutated cells catalyse the reduction of α-KG to 2HG, which drives tumorigenesis and is thus defined as ‘oncometabolite’ [88, 89]. IDH mutations determine significantly better prognosis and are included in the World Health Organization Classification of Central Nervous System Tumours since 2016 as fundamental items. Moreover, target therapies have been developed and are currently being evaluated.

Since 2012, specifically tailored MRS sequences (including PRESS, MEGA-PRESS, 1D LASER, 2D LASER, MEGALASER, STEAM and EPSI) have been implemented to detect and quantify 2HG (2HG-MRS). The difficulty lies in 2HG low concentration and in the 2HG peaks (2.25 and 4.02 ppm) overlapping with more abundant metabolites [78, 90, 91] (Fig. 3). This oncometabolite can be detected by 3 T or higher magnetic strength with intermediate TE. Low cellularity and small lesion volume are important limits of 2HG-MRS.

The above-mentioned techniques evolved and improved their accuracy and nowadays can be effective in characterizing naïve and recurrent gliomas, assessing infiltration and monitoring response to treatment. Even though single-voxel and multivoxel spectroscopy have been successfully used in several studies on glioma patients, 2HG-MRS has not yet been validated for widespread clinical use and it is still limited to a few research centres.

MRS for assessing response to therapy

Pseudoprogression, radiation necrosis and recurrent tumour

Pseudoprogression is a non-tumoral increase in the contrast-enhancing lesion that can occur within 3–6 months after radiotherapy or chemotherapy without significant clinical worsening and it disappears or stabilizes on subsequent MRI without any therapy change. This is a concern for patient management in the clinic and in clinical trials. ^{1}H MRS may diagnose pure pseudoprogression in the rare cases of absence of infiltration, but in the most frequent mix scenario, specific treatment-induced features are lacking [92]. Combined with conventional MRI, the discriminating accuracy of these methodologies has been reported to be as high as 96% when the Cho/NAA, Cho/Cr, diffusion and perfusion parameters are included [93, 94].

Radiation necrosis can occur within the radiation field six months after radiotherapy and it is characterized by irregular ring enhancement without hyper-perfusion, and inconstant oedema. MRS shows substantial Lip peak and harmonic decrease of the other metabolites. A mix scenario with glioma and treatment-related effects is often the rule, and MRS can be useful (as far as perfusion-weighted MRI, detecting metabolic instead of vascular signs) to highlight the presence of glioma within the radiation necrosis (high

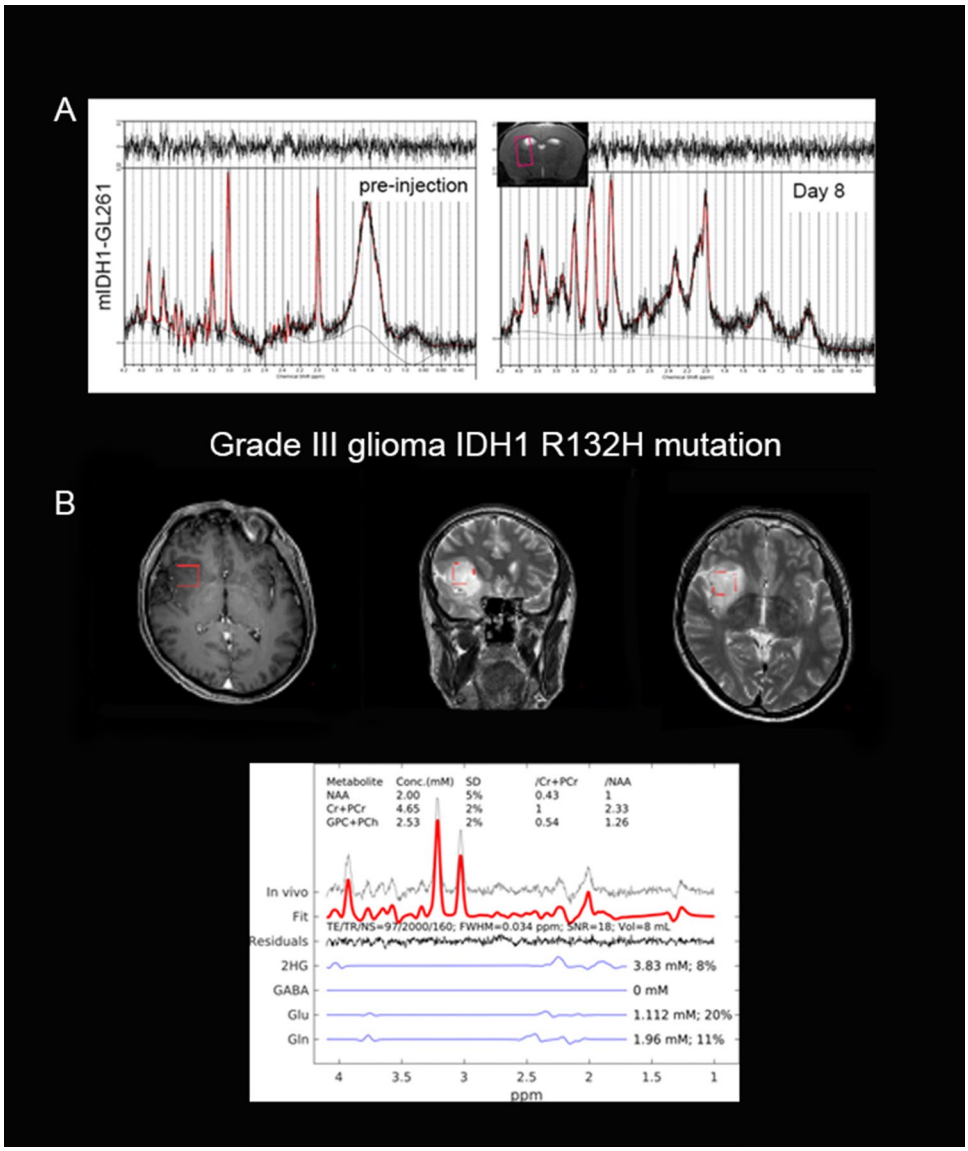

Fig. 3 2HG detection by in vivo brain MRS (tailored PRESS TE = 97 ms single-voxel sequence). **A** 7 T MRS: in xenograft (IDH1-mutant mouse glioma) 2HG peak (2.25 ppm) is absent in healthy brain (left) and detectable when glioma is growing (right) (courtesy of Pellegatta [110]); **B** 3 T MRS: 2HG is quantifiable in an IDH1-mutant glioma human patient

lipids and non-harmonic decrease of the other metabolites with high Cho/NAA) and the glioma infiltration within oedema or gliosis (Fig. 4).

In particular, the post-radiotherapy evolution of the spectral changes associated with Cho compounds is predictive of tumour response: patients with increasing Cho/NAA values during radiotherapy were more likely to progress early [95] while Cho reduction at 2 months post-radiotherapy provide prognostic information regarding progression-free and overall survival [96]. In recurrent gliomas treated with GammaKnife, a reduction of Cho levels and an increase in Lac + Lip concentrations was observed within the radiosurgery target, generally within 6 months after treatment. By contrast, an increase in Cho is associated with a poor outcome, indicating tumour recurrence before new enhancement can be detected [97].

Response to chemotherapies, antiangiogenics, immunotherapy

Twelve months after Temozolomide administration, there were significant reductions in the mean Cho signal in low-grade gliomas [98], whereas at 14 months follow-up a rapid and wide change in MRS profile during early response and later progression was detected, suggesting an early defining characteristic [99].

Among patients with GBM who were treated with antiangiogenics at the time of tumour recurrence, a rise in NAA/Cho levels was associated with a better therapeutic response during the first weeks [100, 101].

During antiangiogenic therapy, Lac can possibly be found in areas where the water diffusivity is reduced, reflecting treatment-related hypoxia rather than tumoral hyper-cellularity and aggressiveness. Moreover, when pseudo-response

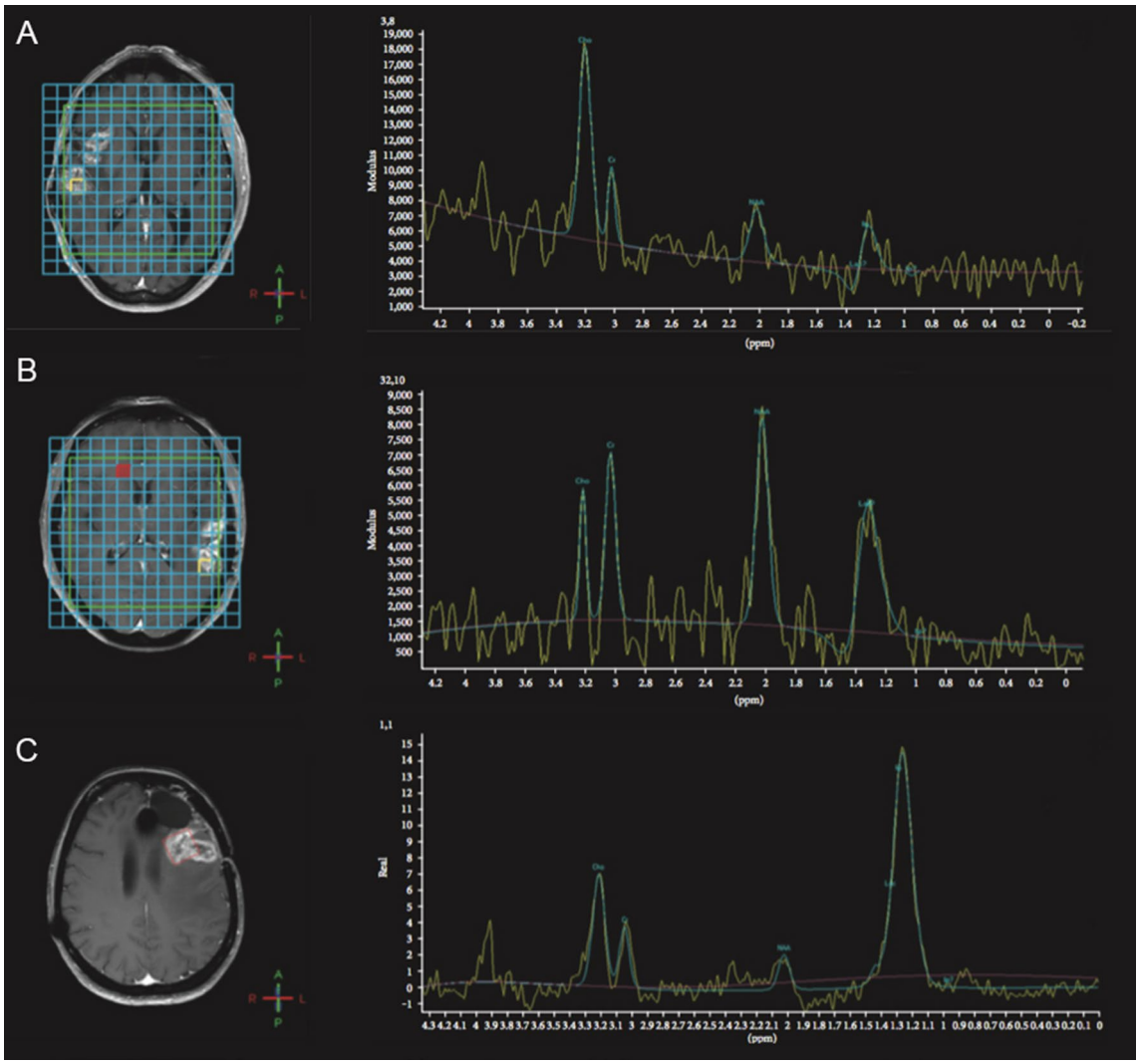

Fig. 4 MRS in necrotic enhancing lesions. **A** MRSI: high Cho/Cr ratio, reduced NAA and small Lipids peak in GBM; **B** MRSI: prominent Lip peak without alteration of the other metabolites' ratios in radiation necrosis; **C** single-voxel MRS: disharmonic reduction of Cho, Cr, NAA and predominant Lip peak suggest the co-existence of high-grade glioma and radiation necrosis

reduces the contrast enhancement but not the tumour itself and perfusion studies are biased by the anti-vascular effect of the treatment, MRS can be useful either to confirm a true response or to evaluate residual or progressing glioma infiltration.

As far as immunotherapy is concerned, lipids have been described as the substrate of natural killer *T*-cells [102] and the presence of an abundant Lip peak might be associated with a better immune response given the relevance of natural killer in immune-responsive GBM receiving immunotherapy with dendritic cells [103].

MRS in pre-clinical research

High-field nuclear magnetic resonance phenomenon benefits from a higher SNR, contrast-to-noise ratio (CNR) and spectral resolution, making it suitable for multiple pre-clinical research applications. Horizontal-bore MRI scanners are commonly employed for preclinical research purposes as they are suitable for a wide variety of samples: cell lines (live cultures or fixed specimens, lysates) [104–106], animal models (typically, rodents like mice and rats) [81, 107], surgical samples or biopsies [108], excreta and micro-dialysates [109]. Animal models are employed engrafting animal tumour lines [110] or as patient-derived xenografts, in which patients' tumour

tissue or cells are implanted into immune-deficient animals [81]. As part of preclinical research, MRS metabolites quantification is used not only to refine diagnostic tools, which can correct for the limitations of Gd-based contrast-enhanced MRI, but also to investigate tumour behaviour and its response to chemo-radiotherapy and advanced therapies.

MRS to improve diagnostic capacity

Since the GBM infiltration zone is difficult to visualize by MRI due to blood–brain barrier incomplete leakage, it poses particular challenges both to diagnosis and treatment targeting. To overcome this issue, Cudalbu and colleagues [111] reported biological features of invasive tumour growth based on transcriptomic and metabolic changes observed in mouse xenografts and in the corresponding patients' tumours. GBM invasion and growth were associated with decreasing neuronal metabolism (GABA, Glu, and NAA) and an increase in cellular turnover specific markers (Cho and mIns). In addition, xenografts metabolite signatures, reflecting temporal changes in tumour evolution, revealed high similarity with metabolite quantifications across patients' tumour areas characterized by different growth and infiltrative behaviours.

Preclinical studies designed to characterize in vivo the IDH1 mutation of GBM xenografts through MRI and MRS resulted in IDH1-mutated tumours exhibiting significant increased NAA, PCr, MIns, Tau concentrations and a decreased concentration of GSH, Glu, Lac and PC as well as the expected increase in 2HG, compared to IDH1-wildtype controls.

MRS to monitor response to therapy

Radiotherapy

GBM is characterized by high resistance to chemo-radiotherapy, mainly due to a surviving fraction of stem-like cells with peculiar metabolic features.

GABA, Glu, Lac, Lip, PCr, and Glucose quantification by ^{1}H MRS contributed to the study of cellular metabolism in GBM stem-like cells with different metabolic and genetic signatures following various radiotherapy interventions [112].

In U87 and C6 glioma cells [106] irradiated with escalating doses of X-rays, in vitro high-resolution MRS showed that the Cho/Cr and Cho/NAA ratios increased after irradiation in a dose-dependent manner. The invasion ability and the number of invading glioma cells also had a high positive correlation with the Cho/Cr and Cho/NAA ratios.

High-field MRS was acquired before irradiation of GBM xenografts in nude mice before and after single fraction radiotherapy: Ala, mIns, Tau, Cr + PCr, Glu + Gln, and total Cho decreased in the short term, followed by an increase 14 days post treatment [113].

IDH-mutations and 2HG

Pellegatta and collaborators [110] evaluated 2HG production in vivo employing ^{1}H MRS absolute quantification in mice bearing R132H IDH1-mutated GL261 gliomas. The findings supported the translational potential of MRS-guided immunotherapeutic targeting of gliomas carrying IDH1 mutations [110].

IDH1 inhibitors AG-881 and BAY-1436032 induced a significant reduction in in vivo 2HG, a significant early and sustained increase in Glu, and a transient early increase in NAA concentration [114]. Moreover, animals had improved survival and metabolic changes were observed before any measurable difference in tumour volume [114].

The phosphoinositide-3-kinase (PI3K)/mammalian target of rapamycin (mTOR) pathway represents another therapeutic target for gliomas with IDH1 mutation, but clear indicators of treatment target modulation are still lacking. Batsios and colleagues [115] tried to identify MRS-detectable metabolic fingerprints associated with IDH1-mutated glioma response to the dual PI3K/mTOR inhibitor XL765. It resulted to induce a significant reduction in different intracellular metabolites, such as 2HG and longer survival following treatment, but without significant inhibition of tumour growth.

As temozolomide is widely administered to patients with IDH1-mutant gliomas, Subramani and colleagues [116] used ^{1}H MRS and hyperpolarized ^{13}C MRS to identify increased Glu production as a potential metabolic biomarker of temozolomide response in genetically engineered and patient-derived models: in temozolomide-treated cells a significant increase in Glu and ^{13}C-Glu levels was observed. Furthermore, in vivo ^{1}H MRS performed in mouse models resulted in an increase of Glu and Gln prior to tumour shrinkage.

GLAST-expressing gliomas and Glu

GLAST (Glutamate-ASpartate Transporter) is expressed by astrocytes and plays a role in Glu uptake [81]. GBM cells heavily express GLAST on their plasma membranes, and its presence correlates with a decreased patient survival rate. Corbetta and colleagues [81] demonstrated that GLAST inhibition by UCPH-101 limited the growth and invasion of GBM xenografts; Glu quantification performed by ^{1}H MRS was shown to predict the infiltrative pattern of high-grade glioma in vivo in murine models, preceding visible progression on conventional MRI [81].

Other therapies

Aberrant histone de-acetylation that silences tumour suppressor genes during carcinogenesis may represent another important therapeutic target for gliomas. SuberoylAnilide Hydroxamic Acid (SAHA) is a well-known inhibitor of histone deacetylase activity but it triggers neoplastic cell re-differentiation and cytostasis rather than tumour size reduction, thus limiting the use of standard imaging techniques. Wei and collaborators [117] investigated the changes in the metabolism induced by an initial response to SAHA treatment in a rat glioma model by ^{1}H MRS: untreated tumours resulted in significantly higher alanine and Lac levels and reduced mIns, NAA, and Cr concentrations.

A potential complementary approach to conventional therapies is interstitial photodynamic therapy, although a suitable treatment scheme still remains under investigation [118]. Nude rats bearing stereotactic-implanted GBM xenografts were treated by interstitial photodynamic therapy, immediately after intravenous injection of photosensitizer agents, and ^{1}H MRS identified Lip, Cho and mIns levels as promising biomarkers to distinguish responders from non-responders.

Ciusani group [119] evaluated the effects of a ketogenic diet on tumour metabolism of a GL261 mouse glioma model by high-field ^{1}H MRS. After implantation, animals were fed standard chow or underwent a ketogenic diet and after 9 days in the ketogenic regime, decreased GABA, NAA, NAAG levels were found in tumour tissue, while a great increase of BHB was detected in the tumour tissue as compared to the normal brain [119].

MRS contrast agents for pre-clinical research

MRS is usually limited to endogenous metabolites. Exogenous MRS contrast agents could improve the specificity and sensitivity of MRS, and the synthesis of new disease-specific contrast agents may lead to molecular imaging improvements even for those tumours "invisible" to standard contrast-enhanced MRI.

β-alanine loaded hollow mesoporous silica nanospheres were synthesized and investigated by Wang et al. [120], resulting in a high biosafety profile and a characteristic spectrum highly sensitive to the MRS diagnosis of glioma.

Delgado-Goñi [121] assessed the contrast agent feasibility of DiMethyl SulfOxide (DMSO), a solvent for chemotherapeutic agents commonly used in preclinical studies on high-grade glioma, in normal brain and in GL261 GBM of C57BL/6 mice by single-voxel MRS to detect brain tumours and monitor their progression or therapeutic response.

X-nuclei MRS

MRS of the so-called X nuclei (especially ^{31}P, ^{13}C, and ^{19}F) is possible with dedicated coils and it is emerging for pre-clinical research broadening in neurology and neuro-oncology [7, 122].

The ^{31}P nucleus is 100% naturally abundant, but being ^{31}P MRS less sensitive than ^{1}H MRS, it requires longer acquisition times and/or larger voxels. Nonetheless, ^{31}P MRS can provide interesting information about ^{31}P-containing metabolites involved in energy and phospholipid pathways, such as PCr, ATP, PC, phosphoethanolamine (PE), and glycerophosphoethanolamine (GPE) [8]. As GBM term refers to a set of heterogeneous tumours, the use of phosphorous MRS may show differences in cellular energy metabolism in the various sub-populations of GBM [123]. EGFR-amplified tumours had significantly lowered PCr/Pi and PCr/ATP ratios, and higher PME/PDE and Pi/ATP which might point out its lower oxidative capacity. The MGMT-methylated tumours resulted in a similar behaviour [123]. Moreover, GBM patients' energetic and membrane metabolism is modified in the entire brain, and ^{31}P MRS may also investigate changes in the presumably "normal-appearing" tissue. This could potentially lead to a more reproducible and reliable non-invasive diagnosis and more individualized therapies [8, 124].

In contrast to ^{1}H- and ^{31}P MRS, the ^{13}C MRS sensitivity is limited by ^{13}C nucleus low natural abundance (1.1%) and low gyromagnetic ratio. Therefore, ^{13}C MRS has to be used after the exogenous infusion of a ^{13}C-labeled contrast agents (CA) [114, 125].The ^{19}F nucleus has a 100% natural abundance and its SNR is about 89% of ^{1}H per nucleus. Since there is negligible endogenous fluorine signal from the body, ^{19}F MRI has a potentially extremely high CNR if a fluorinated contrast agent is introduced even if a very high ^{19}F nuclei density on the molecule and a high tissue concentration are both required to produce a detectable signal. Lai et al. [126] designed a multimodal imaging approach that employed ^{1}H MRS, ^{13}C MRS and ^{18}FDG PET (Positron Emission Tomography) to assess in vivo the metabolism of invasive glioma mouse xenografts. Another group [127] investigated by means of ^{1}H and ^{19}F MRS the 2HG/Cr ratio and the brain penetration of BAY1436032, a fluorine-containing inhibitor of the R132X-mutant IDH1, in IDH1-mutated glioma patients' serum and mice xenografts IDH1.

Hyperpolarized MRS

As small metabolites are present in low concentrations, they may be under the detection limits of conventional MR methods. Efforts to improve the signal by increasing the scanner magnetic field are limited by costs and practical constraints. On the other hand, signal intensity and thus sensitivity could

be enhanced by several orders of magnitude by exploiting different hyperpolarization techniques.

MR signal depends on the slight difference between populations of nuclear spins parallel and anti-parallel to the main magnetic field (polarization), typically in the range of 0.0001 to 0.0005% depending on the nucleus and the applied magnetic field strength. The high concentration of protons in water and fat makes clinical MRI possible despite poor polarization levels. The term hyperpolarization (HP) indicates a significant redistribution of the nuclear spin populations. After hyperpolarization, the signal from a given number of nuclear spins can be raised by a factor of 10,000 or more with respect to equilibrium conditions [128].

Several techniques have been adopted to achieve liquid and gas CA hyperpolarization either completely or on the order of parts per hundred rather than parts per million [129, 130].

Generally, these methods transfer the polarization from easy-polarizable systems to the interested nuclear ensemble. Regardless of the exploited method, the hyperpolarized spin states are unstable, i.e., the induced nonequilibrium decays during a relatively short time.

Among all HP methods, the following are noteworthy in neuro-oncology MRS field. Dynamic Nuclear Polarization (DNP) is based on the transfer of polarization from the unpaired electron spins of paramagnetic centres to neighbouring nuclear spins through dipolar interactions [131]. ParaHydrogen Induced Polarization (PHIP) methods exploit the spin order of the parahydrogen singlet state that can be converted into observable magnetization through fast chemical reactions across unsaturated chemical bonds adjacent to ^{13}C carboxyl or ^{15} N nuclei of the labelled substrate [132]. Finally, Signal Amplification by Reversible Exchange (SABRE) is a relatively new PHIP-based technique that reaches hyperpolarization without changing the chemical identity of the informative agent of interest [133].

DNP and PHIP methods have been used to hyperpolarize injectable molecules containing ^{13}C. To date, the most commonly investigated HP compounds are Pyruvate [125], α-KG [134], and Lac [135]. Several groups exploited hyperpolarized ^{13}C MRS in preclinical and clinical studies to investigate metabolism in healthy brain and neurological diseases. In the context of glioma, several preclinical studies using HP ^{13}C MRS have been successfully conducted [116, 136–140] .

Finally, the hyperpolarization-driven signal enhancement enabled the fast detection of metabolism and real-time imaging of metabolic fluxes, providing a new method to detect tumours and monitor their response to therapy [140].

Application of artificial intelligence

In recent years, several attempts have been made to use the new tools provided by the technological advancement of image analysis and processing software. Artificial Intelligence (AI) algorithms have been known for decades [141, 142] but only the increase in computing power has permitted their application in research and clinical field, even in small centres without the need for major investments in digital hardware. AI requires large amounts of data: hundreds of cases for machine learning and thousands for deep learning [143]. Such data must necessarily (machine learning) or preferably (deep learning) be labelled to be processed by the algorithm. Additionally, considering the different acquisition techniques and the artifacts related to the variability of the single case, all data must be uniformed before being analysed.

In comparison with other fields of radiological application of AI, MRS represents the "Cinderella" of the group: from literature search with keywords "artificial intelligence" AND "MR spectroscopy", a few articles can be found related to glioma studies. The major limitation of MRS studies is the lack of large amounts of data. Although some groups performed experiments on small samples [144, 145], these are not statistically solid because numerical samples of about 50 patients are not sufficient for these methods.

Attempts have been made in using automatic pattern recognition analysis on MR spectra. Using large sets of MRS data and appropriate techniques of features reduction, machine learning algorithms can be trained in a supervised mode to correlate MRS spectra to a defined pathology [146, 147]. The use of pattern-recognition algorithms for the classification and grading of brain tumours has been the subject of debate for at least twenty years [148]. Multicentre experiences with an appropriate number of patients are reported in literature [149–151].

More recently, García-Gómez and colleagues tested the ability of different machine learning algorithms (linear discriminant analysis, least-squares support vector machine, principal component analysis, *K*-nearest neighbours) on single-voxel MRS in differentiating high-grade gliomas, low-grade-gliomas, metastasis and meningiomas, using a large dataset of MRI data from eTUMOR projects including ^{1}H-MRS (about 250 patients) [150]. All pairwise comparisons yielded good results with accuracies around 90%, while the accuracy was less than 78% for GBM versus metastases [150].

Fewer groups have created large datasets of "synthetic" data to overcome the limitations posed by the small sample size using the same computer science techniques. Dikaios [152] used a database of 112 patients (81 GBM and 31 metastases) with both long-TE (using PRESS) and short-TE (using either STEAM and PRESS) MRS acquisitions

from a nodular region where the biopsy was taken to create 31.500 synthetic spectra (six different datasets from two MR machines). A Support Vector Machine (SVM) and Artificial Neural Network (ANN) were used. The author reported a good discrimination power between GBM and metastasis from a combination of short and long TE data (accuracy 0.93, AUC 0.97). In a second attempt to improve MRSI, Iqbal and colleagues [153] used a spectroscopic imaging generator based on UNet [154] to produce high-resolution spectra from not real MRS data. An algorithm was trained from 102.169 MRSI created from a series of 416 open access T1-weighted imaging studies, allowing upsampling of low-resolution spectroscopic images, which can improve the current MRSI workflow.

The application of AI, even including synthetic MRS, is promising but still marginal in the context of MRSI and further steps are needed to create large databases with uniform and comparable data, to unfold the full potential of machine learning in the diagnostic and prognostic prediction of the many central nervous system pathologies that can be investigated with MRS [155].

Limits

Although MRS is useful for in vivo diagnosis and monitoring of gliomas, there are some limitations, first of all the need for detectable metabolites.

Long acquisition times and a lack of standardized analysis [7], limit MRS spread and validation in clinical practice, as do inter-institutional differences in acquisition parameters, field strength, and post-processing algorithms that limit reproducibility [156]. Experts' consensus recommendations can help managing these issues [157].

Tissue heterogeneity, MRS voxel size, lesion volume and localization may affect the local concentration of selective metabolites: normal tissue as far as perifocal oedema, non-viable parts of the tumour, calcifications, cysts, haemorrhage in the voxel and close bone structures may produce artifacts and misleading results.

Finally, MRS is highly sensitive to pathological metabolic changes, but it may be low in specificity without a broader clinical and radiological perspective.

Future directions

Although current MRS research in gliomas is largely focused on the validation and standardization of the detection and quantification of 2HG as a marker for IDH mutations in clinical practice, metabolites related to Gln metabolism can also be detected using that advance neuroimaging technique [7, 158].

Gliomas not only show high glycolysis and Lac production with high glucose needs, but also an increase in Gln intake and storage. Indeed, Gln is catabolized to several by-products that aid cancer proliferation, including Glu and α-KG and it is also a vital nitrogen source for proliferation. Higher Gln catabolism rates are associated to metabolic plasticity, resistance to treatment, and a mesenchymal phenotype. Since mesenchymal subtypes are usually associated with worse outcomes, Gln concentrations may help predicting prognosis. Gln-based PET reported high Gln concentrations in progressing gliomas in comparison with the surrounding brain parenchyma or clinically stable tumours [159]. Moreover, mice treated with chemotherapy showed a significant decrease in tumoral Gln concentrations, thus supporting for the in vivo Gln quantification after the procedure. It has been demonstrated that inhibiting Gln metabolism slows the growth of cancer cells and stimulates antitumor immunity in tumoral microenvironment. Furthermore, since Gln metabolism has been implicated in glioma pathogenesis, this could be a potential pharmacologic target that is being investigated in preclinical and early-stage clinical trials [160, 161].

Translational murine and human studies evaluated GLAST as a target for GBM immunotherapy. GLAST favours the Glu release in the tumour microenvironment and promotes cell migration. Inhibition of GLAST expression impacts cells proliferation and immunization with GLAST peptides induces specific anti-tumour response in the murine model. In vivo Glu quantification is feasible in the human brain with short-echo ^{1}H MRS at 3 T. Glu concentration may predict the infiltrative pattern of high-grade glioma, since Glu is detectable—in patients—within enhancing lesion, higher in perifocal FLAIR hyperintensities, and—in murine models—in the contralateral hemisphere, preceding progression as detectable by conventional MRI [81] (Fig. 5). Noteworthy, lower Glu levels have been demonstrated in IDH-mutated glioma patients with respect to IDH-wildtype [78], the latter known to gain a worse prognosis.

Another valuable marker in the clinical management of gliomas is Gly, a non-essential amino acid and intermediate of nucleotide biosynthesis, that increases with tumour proliferation. Gly can be assessed in glioma patients by single-voxel PRESS sequence with TE of 97 ms [162]. Furthermore, brainstem tumours with elevated Gly levels that did not show post-contrast enhancement at the time of MRS, usually undergo progression shortly after and showed contrast-enhancement at later time points [162]. Findings suggest that Gly metabolism abnormalities could precede blood–brain barrier breakdown, and Gly increase could be considered a prior MRI biomarker of high-grade transformation [162].

Gly and 2HG can be co-detected by MRS at 3 T [162] and a strong association between elevated Gly and Gly/2HG ratio was reported in glioma patients with poor clinical outcome. Therefore, Gly and 2HG MRS tracing may be effective in

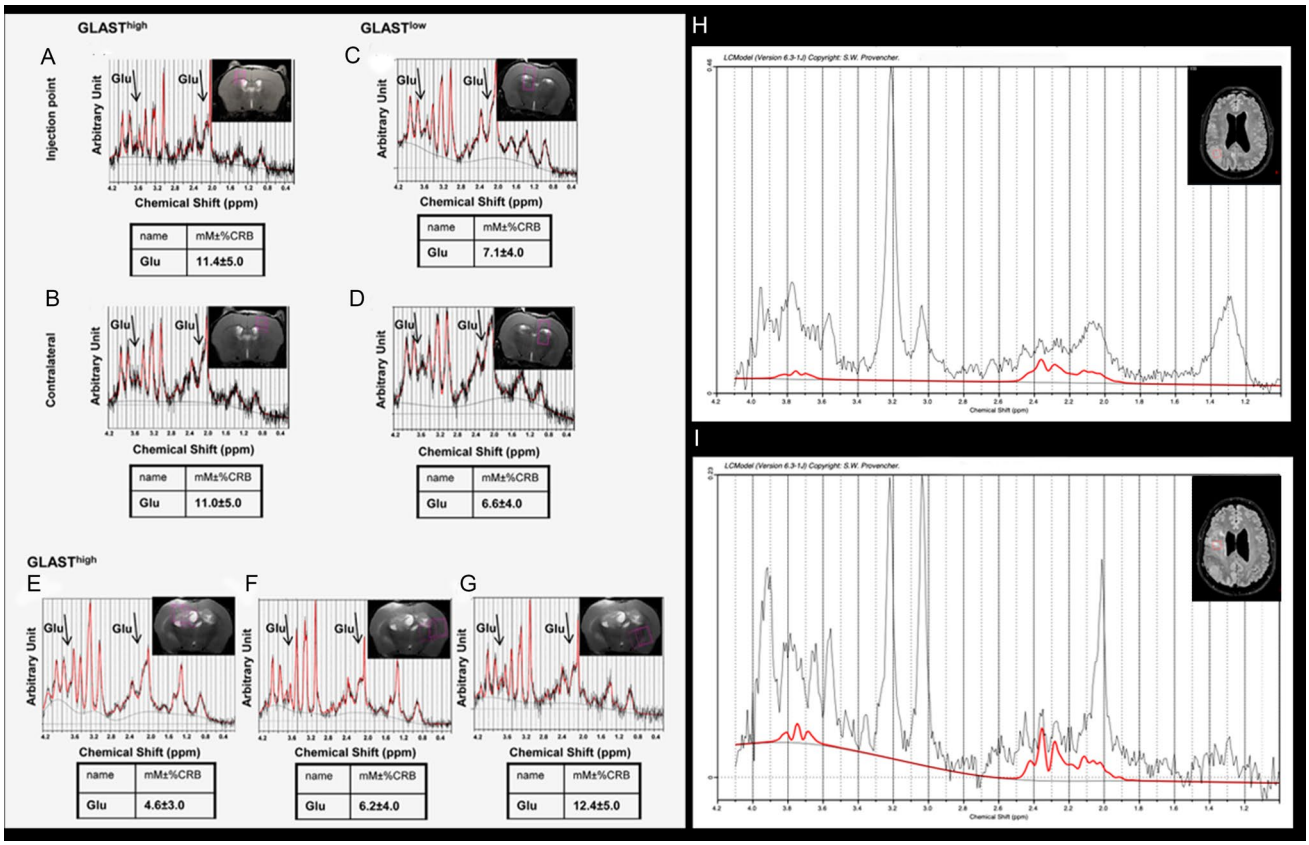

Fig. 5 Glu levels on in vivo brain MRS (tailored PRESS TE = 35 ms single-voxel sequence). Left: murine xenograft GLAST positive (GLAST^{high}) gliomas showed high 7 T MRS Glu levels both within the initial lesion **A** and in the contralateral apparently healthy hemisphere **B** before extensive lesions invaded the contralateral hemisphere (**E**–**G**) with Glu increasing trend from the initial site to contralateral infiltration (courtesy of Corbetta and Pellegatta [81]). Right: 3 T MRS in human high-grade glioma: Glu levels are higher in perilesional infiltration (**I**) than in the main focal lesion (**H**)

identifying aggressively proliferating tumours and predicting patients' survival.

Conclusion

MRS can provide information about tumour metabolic profile. Specific metabolic biomarkers, their quantity and distribution can support glial tumours differential diagnosis. MRS can also recognize the right region of interest in heterogeneous lesions for highly tailored biopsy.

In the context of integrated genomic-histological analysis of brain tumours [1], new biomarkers can provide diagnostic, therapeutic and prognostic information. MRS and MRSI resulted to be a fundamental in vivo neuroimaging technique, able to select target therapies and to predict and assess tumour response through qualitative and quantitative analyses of the brain metabolites.

In conclusion, the characterization of brain tumours through MRS will benefit of a wide synergy among scientists and clinicians of different specialties within the context of new translational competences [163]. Head coils, MRI hardware and post-processing analysis tools progress, advances in research, experts' consensus recommendations and specific professionalizing programs will make the technique increasingly trustworthy, responsive and accessible.

Acknowledgements The authors would like to thank the Italian Ministry of Health for supporting their scientific research.

Author contributions FP: pre-clinical and techniques; FM: pre-clinical and techniques; AE: clinical; LC: clinical; FMD: Artificial intelligence, editing; SP: editing; DA: techniques, editing; MGB: paper concept, future perspectives; VC: paper concept, clinical, oversight; all authors participated to literature review, wrote parts of the manuscript and approved the final text.

Funding The study received no direct funding.

Declarations

Conflict of interest Francesco Padelli, Federica Mazzi, Alessandra Erbetta, Luisa Chiapparini, Sara Palermo, Fabio Martino Doniselli, Domenico Aquino, Maria Grazia Bruzzone, Valeria Cuccarini do not have any conflict of interest to disclose.

Informed consent Not due.

References

1. Louis DN et al (2021) The 2021 WHO classification of tumors of the central nervous system: a summary. Neuro Oncol 23(8):1231–1251. https://doi.org/10.1093/neuonc/noab106
2. Wen PY, Packer RJ (2021) The 2021 WHO classification of tumors of the central nervous system: clinical implications. Neuro Oncol 23(8):1215–1217. https://doi.org/10.1093/neuonc/noab120
3. Pavlova NN, Thompson CB (2016) The emerging hallmarks of cancer metabolism. Cell Metab 23(1):27–47. https://doi.org/10.1016/j.cmet.2015.12.006
4. Huang RY, Lin A (2020) Whole-brain MR spectroscopy imaging of brain tumor metabolites. Radiology 294(3):598–599. https://doi.org/10.1148/radiol.2020192607
5. Caivano R et al (2013) 3 Tesla magnetic resonance spectroscopy: cerebral gliomas vs. metastatic brain tumors. Our experience and review of the literature. Int J Neurosci 123(8):537–543. https://doi.org/10.3109/00207454.2013.774395
6. van Dijken BRJ, van Laar PJ, Holtman GA, van der Hoorn A (2017) Diagnostic accuracy of magnetic resonance imaging techniques for treatment response evaluation in patients with high-grade glioma, a systematic review and meta-analysis. Eur Radiol 27(10):4129–4144. https://doi.org/10.1007/s00330-017-4789-9
7. Ekici S, Nye JA, Neill SG, Allen JW, Shu H-K, Fleischer CC (2022) Glutamine imaging: a new avenue for glioma management. Am J Neuroradiol 43(1):11–18. https://doi.org/10.3174/ajnr.a7333
8. De Graaf RA (2018) In vivo NMR spectroscopy: principles and techniques. Wiley. ISBN: 978-1-119-38251-5
9. Oz G et al (2014) Clinical proton MR spectroscopy in central nervous system disorders. Radiology 270(3):658–679. https://doi.org/10.1148/radiol.13130531
10. Hafez H, Elmoneim BA, Fawzy T, Omar SF (2016) The role of proton magnetic resonance spectroscopy in grading of brain gliomas. Menoufia Med J 29(1):136. https://doi.org/10.4103/1110-2098.179004
11. Bottomley PA (1987) Spatial localization in NMR spectroscopy in vivo. Ann N Y Acad Sci 508(1):333–348. https://doi.org/10.1111/J.1749-6632.1987.TB32915.X
12. Frahm J, Merboldt K-D, Hänicke W (1987) Localized proton spectroscopy using stimulated echoes. J Magn Reson 72(3):502–508. https://doi.org/10.1016/0022-2364(87)90154-5
13. Moonen CT et al (1989) Comparison of single-shot localization methods (STEAM and PRESS) for in vivo proton NMR spectroscopy. NMR Biomed 2(5–6):201–208. https://doi.org/10.1002/nbm.1940020506
14. Zhu H, Barker PB (2011) MR spectroscopy and spectroscopic imaging of the brain. Methods Mol Biol 711:203–226. https://doi.org/10.1007/978-1-61737-992-5_9
15. Garwood M, DelaBarre L (2001) The Return of the frequency sweep: designing adiabatic pulses for contemporary NMR. J Magn Reson 153(2):155–177. https://doi.org/10.1006/jmre.2001.2340
16. Öz G et al (2021) Advanced single voxel 1 H magnetic resonance spectroscopy techniques in humans: experts' consensus recommendations. NMR Biomed. https://doi.org/10.1002/nbm.4236
17. Oz G, Tkáč I (2011) Short-echo, single-shot, full-intensity proton magnetic resonance spectroscopy for neurochemical profiling at 4 T: validation in the cerebellum and brainstem. Magn Reson Med 65(4):901–910. https://doi.org/10.1002/mrm.22708
18. Lin M, Kumar A, Yang S (2014) Two-dimensional J-resolved LASER and semi-LASER spectroscopy of human brain. Magn Reson Med 71(3):911–920. https://doi.org/10.1002/mrm.24732
19. Slotboom J, Mehlkopf A, Bovée WMM (1991) A single-shot localization pulse sequence suited for coils with inhomogeneous RF fields using adiabatic slice-selective RF pulses. J Magn Reson 95(2):396–404. https://doi.org/10.1016/0022-2364(91)90229-M
20. Mlynárik V, Gambarota G, Frenkel H, Gruetter R (2006) Localized short-echo-time proton MR spectroscopy with full signal-intensity acquisition. Magn Reson Med 56(5):965–970. https://doi.org/10.1002/mrm.21043
21. Brown TR, Kincaid BM, Ugurbil K (1982) NMR chemical shift imaging in three dimensions. Proc Natl Acad Sci 79(11):3523–3526. https://doi.org/10.1073/pnas.79.11.3523
22. Puri BK, Egan M, Wallis F, Jakeman P (2018) Repeatability of two-dimensional chemical shift imaging multivoxel proton magnetic resonance spectroscopy for measuring human cerebral choline-containing compounds. World J Psychiatry 8(1):20–26. https://doi.org/10.5498/wjp.v8.i1.20
23. Bendini M et al (2011) Primary and metastatic intraaxial brain tumors: prospective comparison of multivoxel 2D chemical-shift imaging (CSI) proton MR spectroscopy, perfusion MRI, and histopathological findings in a group of 159 patients. Acta Neurochir (Wien) 153(2):403–412. https://doi.org/10.1007/s00701-010-0833-0
24. Posse S, Otazo R, Dager SR, Alger J (2013) MR spectroscopic imaging: principles and recent advances. J Magn Reson Imaging 37(6):1301–1325. https://doi.org/10.1002/jmri.23945
25. Vidya Shankar R, Chang JC, Hu HH, Kodibagkar VD (2019) Fast data acquisition techniques in magnetic resonance spectroscopic imaging. NMR Biomed 32(3):1–22. https://doi.org/10.1002/nbm.4046
26. Tsai SY, Lin YR, Wang WC, Niddam DM (2012) Short- and long-term quantitation reproducibility of brain metabolites in the medial wall using proton echo planar spectroscopic imaging. Neuroimage 63(3):1020–1029. https://doi.org/10.1016/j.neuroimage.2012.07.039
27. Adalsteinsson E, Irarrazabal P, Topp S, Meyer C, Macovski A, Spielman DM (1998) Volumetric spectroscopic imaging with spiral-based k-space trajectories. Magn Reson Med 39(6):889–898. https://doi.org/10.1002/mrm.1910390606

28. Mayer D, Kim D-H, Spielman DM, Bammer R (2008) Fast parallel spiral chemical shift imaging at 3T using iterative SENSE reconstruction. Magn Reson Med 59(4):891–897. https://doi.org/10.1002/mrm.21572
29. Bogner W, Otazo R, Henning A (2021) Accelerated MR spectroscopic imaging-a review of current and emerging techniques. NMR Biomed 34(5):e4314. https://doi.org/10.1002/nbm.4314
30. Bogner W et al (2014) 3D GABA imaging with real-time motion correction, shim update and reacquisition of adiabatic spiral MRSI. Neuroimage 103:290–302. https://doi.org/10.1016/j.neuroimage.2014.09.032
31. Jafari-Khouzani K et al (2016) Volumetric relationship between 2-hydroxyglutarate and FLAIR hyperintensity has potential implications for radiotherapy planning of mutant IDH glioma patients. Neuro Oncol 18(11):1569–1578. https://doi.org/10.1093/neuonc/now100
32. Waugh JS (1988) Principles of nuclear magnetic resonance in one and two dimensions, R. R. Ernst, G. Bodenhausen, and A. Wokaun Oxford University Press, London/New York 1987. 610 pp. $98. Magn Reson Med 7(2):253–253. https://doi.org/10.1002/mrm.1910070215
33. Leather T, Jenkinson MD, Das K, Poptani H (2017) Magnetic resonance spectroscopy for detection of 2-hydroxyglutarate as a biomarker for IDH mutation in gliomas. Metabolites. https://doi.org/10.3390/metabo7020029
34. Buonocore MH, Maddock RJ (2015) Magnetic resonance spectroscopy of the brain: a review of physical principles and technical methods. Rev Neurosci 26(6):609–632. https://doi.org/10.1515/revneuro-2015-0010
35. Andronesi OC et al (2012) Detection of 2-hydroxyglutarate in IDH-mutated glioma patients by in vivo spectral-editing and 2D correlation magnetic resonance spectroscopy. Sci Transl Med. https://doi.org/10.1126/scitranslmed.3002693
36. Mescher M, Tannus A, O'Neil Johnson M, Garwood M (1996) Solvent suppression using selective echo dephasing. J Magn Reson Ser A 123(2):226–229. https://doi.org/10.1006/jmra.1996.0242
37. Mescher M, Merkle H, Kirsch J, Garwood M, Gruetter R (1998) Simultaneous in vivo spectral editing and water suppression. NMR Biomed 11(6):266–272. https://doi.org/10.1002/(sici)1099-1492(199810)11:6%3c266::aid-nbm530%3e3.0.co;2-j
38. Mullins PG et al (2014) Current practice in the use of MEGA-PRESS spectroscopy for the detection of GABA. Neuroimage 86:43–52. https://doi.org/10.1016/J.NEUROIMAGE.2012.12.004
39. Branzoli F et al (2018) Highly specific determination of IDH status using edited in vivo magnetic resonance spectroscopy. Neuro Oncol 20(7):907–916. https://doi.org/10.1093/neuonc/nox214
40. Frahm J, Bruhn H, Gyngell ML, Merboldt KD, Hänicke W, Sauter R (1989) Localized high-resolution proton NMR spectroscopy using stimulated echoes: Initial applications to human brain in vivo. Magn Reson Med 9(1):79–93. https://doi.org/10.1002/mrm.1910090110
41. Ogg RJ, Kingsley PB, Taylor JS (1994) WET, a T1- and B1-insensitive water-suppression method for in vivo localized 1H NMR spectroscopy. J Magn Reson B 104(1):1–10. https://doi.org/10.1006/JMRB.1994.1048
42. Tkáč I, Gruetter R (2005) Methodology of H NMR spectroscopy of the human brain at very high magnetic fields. Appl Magn Reson 29(1):139–157. https://doi.org/10.1007/BF03166960
43. De Graaf RA, Nicolay K (1998) Adiabatic water suppression using frequency selective excitation. Magn Reson Med 40(5):690–696. https://doi.org/10.1002/mrm.1910400508
44. Tkáč I et al (2021) Water and lipid suppression techniques for advanced 1 H MRS and MRSI of the human brain: experts' consensus recommendations. NMR Biomed. https://doi.org/10.1002/nbm.4459
45. Bogner W, Otazo R, Henning A (2021) Accelerated MR spectroscopic imaging—a review of current and emerging techniques. NMR Biomed 34(5):1–32. https://doi.org/10.1002/nbm.4314
46. Miller KL, Tijssen RH, Stikov N, Okell TW (2011) Steady-state MRI: methods for neuroimaging. Imaging Med 3(1):93–105. https://doi.org/10.2217/IIM.10.66
47. Althaus M, Dreher W, Geppert C, Leibfritz D (2006) Fast 3D echo planar SSFP-based 1H spectroscopic imaging: demonstration on the rat brain in vivo. Magn Reson Imaging 24(5):549–555. https://doi.org/10.1016/j.mri.2005.09.015
48. Dreher W, Erhard P, Leibfritz D (2011) Fast three-dimensional proton spectroscopic imaging of the human brain at 3 T by combining spectroscopic missing pulse steady-state free precession and echo planar spectroscopic imaging. Magn Reson Med 66(6):1518–1525. https://doi.org/10.1002/mrm.22963
49. Duyn JH, Moonen CTW (1993) Fast proton spectroscopic imaging of human brain using multiple spin-echoes. Magn Reson Med 30(4):409–414. https://doi.org/10.1002/mrm.1910300403
50. Banerjee S, Ozturk-Isik E, Nelson SJ, Majumdar S (2009) Elliptical magnetic resonance spectroscopic imaging with GRAPPA for imaging brain tumors at 3 T. Magn Reson Imaging 27(10):1319–1325. https://doi.org/10.1016/j.mri.2009.05.031
51. Hamilton J, Franson D, Seiberlich N (2017) Recent advances in parallel imaging for MRI. Prog Nucl Magn Reson Spectrosc 101:71–95. https://doi.org/10.1016/j.pnmrs.2017.04.002
52. Feinberg DA, Setsompop K (2013) Ultra-fast MRI of the human brain with simultaneous multi-slice imaging. J Magn Reson 229:90–100. https://doi.org/10.1016/j.jmr.2013.02.002
53. Geethanath S et al (2012) Compressive sensing could accelerate 1H MR metabolic imaging in the clinic. Radiology 262(3):985–994. https://doi.org/10.1148/radiol.11111098
54. Hu X, Levin DN, Lauterbur PC, Spraggins T (1988) SLIM: spectral localization by imaging. Magn Reson Med 8(3):314–322. https://doi.org/10.1002/mrm.1910080308
55. Zhang Y, Gabr RE, Zhou J, Weiss RG, Bottomley PA (2013) Highly-accelerated quantitative 2D and 3D localized spectroscopy with linear algebraic modeling (SLAM) and sensitivity encoding. J Magn Reson 237:125–138. https://doi.org/10.1016/j.jmr.2013.09.018
56. Lam F, Ma C, Clifford B, Johnson CL, Liang ZP (2016) High-resolution (1) H-MRSI of the brain using SPICE: Data acquisition and image reconstruction. Magn Reson Med 76(4):1059–1070. https://doi.org/10.1002/MRM.26019
57. Ma C, Lam F, Ning Q, Johnson CL, Liang ZP (2017) High-resolution 1 H-MRSI of the brain using short-TE SPICE. Magn Reson Med 77(2):467–479. https://doi.org/10.1002/MRM.26130
58. Chaumeil MM, Lupo JM, Ronen SM (2015) Magnetic resonance (MR) metabolic imaging in glioma. Brain Pathol 25(6):769–780. https://doi.org/10.1111/bpa.12310
59. Jansen JFA, Backes WH, Nicolay K, Kooi ME (2006) 1H MR spectroscopy of the brain: absolute quantification of metabolites. Radiology 240(2):318–332. https://doi.org/10.1148/radiol.2402050314
60. Stagg CJ, Rothman DL (2013) Magnetic resonance spectroscopy: tools for neuroscience research and emerging clinical applications. Magn Reson Spectrosc Tools Neurosci Res Emerg Clin Appl. https://doi.org/10.1016/C2011-0-09647-3
61. Meyer RA, Fisher MJ, Nelson SJ, Brown TR (1988) Evaluation of manual methods for integration ofin vivo phosphorus NMR spectra. NMR Biomed 1(3):131–135. https://doi.org/10.1002/nbm.1940010306
62. Near J et al (2021) Preprocessing, analysis and quantification in single-voxel magnetic resonance spectroscopy: experts'

consensus recommendations. NMR Biomed 34(5):1–23. https://doi.org/10.1002/nbm.4257
63. Mandal PK (2012) In vivo proton magnetic resonance spectroscopic signal processing for the absolute quantitation of brain metabolites. Eur J Radiol 81(4):e653–e664. https://doi.org/10.1016/j.ejrad.2011.03.076
64. Stefan D et al (2009) Quantitation of magnetic resonance spectroscopy signals: the jMRUI software package. Meas Sci Technol. https://doi.org/10.1088/0957-0233/20/10/104035
65. Provencher SW (1993) Estimation of metabolite concentrations from localized in vivo proton NMR spectra. Magn Reson Med 30(6):672–679. https://doi.org/10.1002/mrm.1910300604
66. Gajdošík M, Landheer K, Swanberg KM, Juchem C (2021) INSPECTOR: free software for magnetic resonance spectroscopy data inspection, processing, simulation and analysis. Sci Rep 11(1):1–16. https://doi.org/10.1038/s41598-021-81193-9
67. Dowling C et al (2001) Preoperative proton MR spectroscopic imaging of brain tumors: correlation with histopathologic analysis of resection specimens. AJNR Am J Neuroradiol 22(4):604–612
68. Bulik M, Jancalek R, Vanicek J, Skoch A, Mechl M (2013) Potential of MR spectroscopy for assessment of glioma grading. Clin Neurol Neurosurg 115(2):146–153. https://doi.org/10.1016/J.CLINEURO.2012.11.002
69. Chang J, Thakur SB, Huang W, Narayana A (2008) Magnetic resonance spectroscopy imaging (MRSI) and brain functional magnetic resonance imaging (fMRI) for radiotherapy treatment planning of glioma. Technol Cancer Res Treat 7(5):349–362
70. Hlaihel C, Guilloton L, Guyotat J, Streichenberger N, Honnorat J, Cotton F (2010) Predictive value of multimodality MRI using conventional, perfusion, and spectroscopy MR in anaplastic transformation of low-grade oligodendrogliomas. J Neurooncol 97(1):73–80. https://doi.org/10.1007/S11060-009-9991-4
71. Hattingen E et al (2008) Prognostic value of choline and creatine in WHO grade II gliomas. Neuroradiology 50(9):759–767. https://doi.org/10.1007/S00234-008-0409-3
72. Law M (2004) MR spectroscopy of brain tumors. Top Magn Reson Imaging 15(5):291–313. https://doi.org/10.1097/00002142-200410000-00003
73. Cuccarini V et al (2016) Advanced MRI may complement histological diagnosis of lower grade gliomas and help in predicting survival. J Neurooncol 126(2):279–288. https://doi.org/10.1007/S11060-015-1960-5
74. McKnight TR (2004) Proton magnetic resonance spectroscopic evaluation of brain tumor metabolism. Semin Oncol 31(5):605–617. https://doi.org/10.1053/J.SEMINONCOL.2004.07.003
75. Nelson SJ (2011) Assessment of therapeutic response and treatment planning for brain tumors using metabolic and physiological MRI. NMR Biomed 24(6):734–749. https://doi.org/10.1002/NBM.1669
76. Nelson SJ (2003) Multivoxel magnetic resonance spectroscopy of brain tumors. Mol Cancer Ther 2(5):497–507
77. Ricard D et al (2007) Dynamic history of low-grade gliomas before and after temozolomide treatment. Ann Neurol 61(5):484–490. https://doi.org/10.1002/ana.21125
78. Cuccarini V et al (2020) In vivo 2-hydroxyglutarate-proton magnetic resonance spectroscopy (3 T, PRESS technique) in treatment-naïve suspect lower-grade gliomas: feasibility and accuracy in a clinical setting. Neurol Sci 41(2):347–355. https://doi.org/10.1007/S10072-019-04087-9
79. Li Y et al (2015) Short-echo three-dimensional H-1 MR spectroscopic imaging of patients with glioma at 7 Tesla for characterization of differences in metabolite levels. J Magn Reson Imaging 41(5):1332–1341. https://doi.org/10.1002/JMRI.24672
80. Wright AJ, Fellows GA, Griffiths JR, Wilson M, Bell BA, Howe FA (2010) Ex-vivo HRMAS of adult brain tumours: metabolite quantification and assignment of tumour biomarkers. Mol Cancer. https://doi.org/10.1186/1476-4598-9-66
81. Corbetta C et al (2019) Altered function of the glutamate–aspartate transporter GLAST, a potential therapeutic target in glioblastoma. Int J Cancer 144(10):2539–2554. https://doi.org/10.1002/ijc.31985
82. Ruiz J, Lesser GJ (2009) Low-grade gliomas. Curr Treat Options Oncol 10(3–4):231–242. https://doi.org/10.1007/S11864-009-0096-2
83. Lang FF, Gilbert MR (2006) Diffusely infiltrative low-grade gliomas in adults. J Clin Oncol 24(8):1236–1245. https://doi.org/10.1200/JCO.2005.05.2399
84. Jenkinson MD et al (2005) MRS of oligodendroglial tumors: correlation with histopathology and genetic subtypes. Neurology 64(12):2085–2089. https://doi.org/10.1212/01.WNL.0000165998.73779.D9
85. Jaskólski DJ et al (2013) Magnetic resonance spectroscopy in intracranial tumours of glial origin. Neurol Neurochir Pol 47(5):438–449. https://doi.org/10.5114/NINP.2013.32999
86. Chawla S et al (2010) Role of proton magnetic resonance spectroscopy in differentiating oligodendrogliomas from astrocytomas. J Neuroimaging 20(1):3–8. https://doi.org/10.1111/J.1552-6569.2008.00307.X
87. Branzoli F et al (2019) Cystathionine as a marker for 1p/19q codeleted gliomas by in vivo magnetic resonance spectroscopy. Neuro Oncol 21(6):765–774. https://doi.org/10.1093/neuonc/noz031
88. Prensner JR, Chinnaiyan AM (2011) Metabolism unhinged: IDH mutations in cancer. Nat Med 17(3):291–293. https://doi.org/10.1038/nm0311-291
89. Yan H et al (2009) IDH1 and IDH2 mutations in gliomas. N Engl J Med 360(8):765–773. https://doi.org/10.1056/NEJMOA0808710
90. Choi C et al (2012) 2-hydroxyglutarate detection by magnetic resonance spectroscopy in IDH-mutated patients with gliomas. Nat Med 18(4):624–629. https://doi.org/10.1038/NM.2682
91. Ganji SK et al (2017) In vivo detection of 2-hydroxyglutarate in brain tumors by optimized point-resolved spectroscopy (PRESS) at 7T. Magn Reson Med 77(3):936–944. https://doi.org/10.1002/MRM.26190
92. Alimenti A et al (2007) Monovoxel 1H magnetic resonance spectroscopy in the progression of gliomas. Eur Neurol 58(4):198–209. https://doi.org/10.1159/000107940
93. Di Costanzo A et al (2014) Recurrent glioblastoma multiforme versus radiation injury: a multiparametric 3-T MR approach. Radiol Med 119(8):616–624. https://doi.org/10.1007/S11547-013-0371-Y
94. Zeng QS, Li CF, Liu H, Zhen JH, Feng DC (2007) Distinction between recurrent glioma and radiation injury using magnetic resonance spectroscopy in combination with diffusion-weighted imaging. Int J Radiat Oncol Biol Phys 68(1):151–158. https://doi.org/10.1016/J.IJROBP.2006.12.001
95. Muruganandham M et al (2014) 3-Dimensional magnetic resonance spectroscopic imaging at 3 Tesla for early response assessment of glioblastoma patients during external beam radiation therapy. Int J Radiat Oncol Biol Phys 90(1):181–189. https://doi.org/10.1016/J.IJROBP.2014.05.014
96. Quon H et al (2011) Changes in serial magnetic resonance spectroscopy predict outcome in high-grade glioma during and after postoperative radiotherapy. Anticancer Res 31(10):3559–3565
97. Graves EE et al (2001) Serial proton MR spectroscopic imaging of recurrent malignant gliomas after gamma knife radiosurgery. AJNR Am J Neuroradiol 22(4):613–624

98. Murphy PS et al (2004) Monitoring temozolomide treatment of low-grade glioma with proton magnetic resonance spectroscopy. Br J Cancer 90(4):781–786. https://doi.org/10.1038/SJ.BJC.6601593
99. Guillevin R et al (2011) Predicting the outcome of grade II glioma treated with temozolomide using proton magnetic resonance spectroscopy. Br J Cancer 104(12):1854–1861. https://doi.org/10.1038/BJC.2011.174
100. Ratai EM et al (2013) Magnetic resonance spectroscopy as an early indicator of response to anti-angiogenic therapy in patients with recurrent glioblastoma: RTOG 0625/ACRIN 6677. Neuro Oncol 15(7):936–944. https://doi.org/10.1093/NEUONC/NOT044
101. Kim H et al (2011) Serial magnetic resonance spectroscopy reveals a direct metabolic effect of cediranib in glioblastoma. Cancer Res 71(11):3745–3752. https://doi.org/10.1158/0008-5472.CAN-10-2991
102. Lawson V (2012) Turned on by danger: activation of CD1d-restricted invariant natural killer T cells. Immunology 137(1):20. https://doi.org/10.1111/J.1365-2567.2012.03612.X
103. Pellegatta S et al (2013) The natural killer cell response and tumor debulking are associated with prolonged survival in recurrent glioblastoma patients receiving dendritic cells loaded with autologous tumor lysates. Oncoimmunology. https://doi.org/10.4161/ONCI.23401
104. Mirbahai L et al (2011) 1H magnetic resonance spectroscopy metabolites as biomarkers for cell cycle arrest and cell death in rat glioma cells. Int J Biochem Cell Biol 43(7):990–1001. https://doi.org/10.1016/j.biocel.2010.07.002
105. Grande S et al (2018) Metabolic heterogeneity evidenced by MRS among patient-derived glioblastoma multiforme stem-like cells accounts for cell clustering and different responses to drugs. Stem Cells Int. https://doi.org/10.1155/2018/3292704
106. Xu Y-J et al (2016) Noninvasive evaluation of radiation-enhanced glioma cells invasiveness by ultra-high-field 1H-MRS in vitro. Magn Reson Imaging 34(8):1121–1127. https://doi.org/10.1016/j.mri.2016.05.009
107. Clément A et al (2021) In vivo characterization of physiological and metabolic changes related to isocitrate dehydrogenase 1 mutation expcression by multiparametric MRI and MRS in a rat model with orthotopically grafted human-derived glioblastoma cell lines. NMR Biomed 34(6):1–11. https://doi.org/10.1002/nbm.4490
108. Lucas-Torres C, Roumes H, Bouchaud V, Bouzier-Sore A, Wong A (2021) Metabolic NMR mapping with microgram tissue biopsy. NMR Biomed. https://doi.org/10.1002/nbm.4477
109. Glöggler S et al (2016) In vivo online magnetic resonance quantification of absolute metabolite concentrations in microdialysate. Sci Rep 6(April):6–13. https://doi.org/10.1038/srep36080
110. Pellegatta S et al (2015) Effective immuno-targeting of the IDH1 mutation R132H in a murine model of intracranial glioma. Acta Neuropathol Commun 3:4. https://doi.org/10.1186/s40478-014-0180-0
111. Cudalbu C et al (2021) Metabolic and transcriptomic profiles of glioblastoma invasion revealed by comparisons between patients and corresponding orthotopic xenografts in mice. Acta Neuropathol Commun 9(1):1–16. https://doi.org/10.1186/s40478-021-01232-4
112. Palma A et al (2020) Different mechanisms underlie the metabolic response of GBM stem-like cells to ionizing radiation: Biological and MRS studies on effects of photons and carbon ions. Int J Mol Sci 21(14):1–18. https://doi.org/10.3390/ijms21145167
113. Tessier AG, Yahya A, Larocque MP, Fallone BG, Syme A (2014) Longitudinal evaluation of the metabolic response of a tumor xenograft model to single fraction radiation therapy using magnetic resonance spectroscopy. Phys Med Biol 59(17):5061–5072. https://doi.org/10.1088/0031-9155/59/17/5061
114. Radoul M et al (2021) Early noninvasive metabolic biomarkers of mutant idh inhibition in glioma. Metabolites 11(2):1–17. https://doi.org/10.3390/metabo11020109
115. Batsios G et al (2019) PI3K/mTOR inhibition of IDH1 mutant glioma leads to reduced 2HG production that is associated with increased survival. Sci Rep 9(1):1–15. https://doi.org/10.1038/s41598-019-47021-x
116. Subramani E et al (2020) Glutamate is a noninvasive metabolic biomarker of IDH1-mutant glioma response to temozolomide treatment. Cancer Res 80(22):5098–5108. https://doi.org/10.1158/0008-5472.CAN-20-1314
117. Wei L et al (2012) Early prediction of response to vorinostat in an orthotopic rat glioma model. NMR Biomed 25(9):1104–1111. https://doi.org/10.1002/nbm.2776
118. Toussaint M et al (2017) Proton MR spectroscopy and diffusion MR imaging monitoring to predict tumor response to interstitial photodynamic therapy for glioblastoma. Theranostics 7(2):436–451. https://doi.org/10.7150/thno.17218
119. Ciusani E et al (2021) MR-spectroscopy and survival in mice with high grade glioma undergoing unrestricted ketogenic diet. Nutr Cancer 73(11–12):2315–2322. https://doi.org/10.1080/01635581.2020.1822423
120. Wang J et al (2018) Exogenous amino acid-loaded nanovehicles: stepping across endogenous magnetic resonance spectroscopy. Adv Healthc Mater. https://doi.org/10.1002/adhm.201800317
121. Delgado-Goñi T, Martín-Sitjar J, Simões RV, Acosta M, Lope-Piedrafita S, Arús C (2013) Dimethyl sulfoxide (DMSO) as a potential contrast agent for brain tumors. NMR Biomed 26(2):173–184. https://doi.org/10.1002/nbm.2832
122. Fulham MJ et al (1992) Mapping of brain tumor metabolites with proton MR spectroscopic imaging: clinical relevance. Radiology 185(3):675–686. https://doi.org/10.1148/RADIOLOGY.185.3.1438744
123. Galijašević M et al (2021) Phosphorous magnetic resonance spectroscopy and molecular markers in IDH1 wild type glioblastoma. Cancers (Basel). https://doi.org/10.3390/CANCERS13143569
124. Grams AE et al (2021) Changes in brain energy and membrane metabolism in glioblastoma following chemoradiation. Curr Oncol 28(6):5041–5053. https://doi.org/10.3390/curroncol28060424
125. Izquierdo-Garcia JL et al (2015) IDH1 mutation induces reprogramming of pyruvate metabolism. Cancer Res 75(15):2999–3009. https://doi.org/10.1158/0008-5472.CAN-15-0840
126. Lai M et al (2018) In vivo characterization of brain metabolism by 1H MRS, 13C MRS and 18FDG PET reveals significant glucose oxidation of invasively growing glioma cells. Int J Cancer 143(1):127–138. https://doi.org/10.1002/ijc.31299
127. Wenger KJ et al (2020) Non-invasive measurement of drug and 2-HG signals using19F and1H MR spectroscopy in brain tumors treated with the mutant IDH1 inhibitor bay1436032. Cancers (Basel) 12(11):1–11. https://doi.org/10.3390/cancers12113175
128. Kurhanewicz J et al (2011) Analysis of cancer metabolism by imaging hyperpolarized nuclei: prospects for translation to clinical research. Neoplasia 13(2):81–97. https://doi.org/10.1593/neo.101102
129. Nikolaou P, Goodson BM, Chekmenev EY (2015) NMR hyperpolarization techniques for biomedicine. Chemistry 21(8):3156–3166. https://doi.org/10.1002/chem.201405253
130. Kovtunov KV et al (2018) Hyperpolarized NMR spectroscopy: d -DNP, PHIP, and SABRE techniques. Chem An Asian J 13(15):1857–1871. https://doi.org/10.1002/asia.201800551

131. Ardenkjær-Larsen JH et al (2003) Increase in signal-to-noise ratio of >10,000 times in liquid-state NMR. Proc Natl Acad Sci U S A 100(18):10158–10163. https://doi.org/10.1073/pnas.1733835100
132. Bowers CR, Weitekamp DP (1987) Parahydrogen and synthesis allow dramatically enhanced nuclear alignment. J Am Chem Soc 109(18):5541–5542. https://doi.org/10.1021/ja00252a049
133. Adams RW et al (2009) Reversible interactions with para-hydrogen enhance NMR sensitivity by polarization transfer. Science (80-) 323(5922):1708–1711. https://doi.org/10.1126/science.1168877
134. Molloy AR et al (2020) MR-detectable metabolic biomarkers of response to mutant IDH inhibition in low-grade glioma. Theranostics 10(19):8757–8770. https://doi.org/10.7150/thno.47317
135. Venkatesh HS, Chaumeil MM, Ward CS, Haas-Kogan DA, James CD, Ronen SM (2012) Reduced phosphocholine and hyperpolarized lactate provide magnetic resonance biomarkers of PI3K/Akt/mTOR inhibition in glioblastoma. Neuro Oncol 14(3):315–325. https://doi.org/10.1093/neuonc/nor209
136. Grist JT et al (2020) Hyperpolarized 13C MRI: a novel approach for probing cerebral metabolism in health and neurological disease. J Cereb Blood Flow Metab 40(6):1137–1147. https://doi.org/10.1177/0271678X20909045
137. Hu J, Salzillo TC, Sailasuta N, Lang FF, Bhattacharya P (2017) Interrogating IDH mutation in brain tumor: magnetic resonance and hyperpolarization. Top Magn Reson Imaging 26(1):27–32. https://doi.org/10.1097/RMR.0000000000000113
138. Park I et al (2010) Hyperpolarized 13C magnetic resonance metabolic imaging: application to brain tumors. Neuro Oncol 12(2):133–144. https://doi.org/10.1093/neuonc/nop043
139. Brindle KM, Bohndiek SE, Gallagher FA, Kettunen MI (2011) Tumor imaging using hyperpolarized 13C magnetic resonance spectroscopy. Magn Reson Med 66(2):505–519. https://doi.org/10.1002/mrm.22999
140. Najac C, Ronen SM (2016) MR molecular imaging of brain cancer metabolism using hyperpolarized 13C magnetic resonance spectroscopy. Top Magn Reson Imaging 25(5):187–196. https://doi.org/10.1097/RMR.0000000000000104
141. Conners RW, Harlow CA (1980) A theoretical comparison of texture algorithms. IEEE Trans Pattern Anal Mach Intell 2(3):204–222. https://doi.org/10.1109/TPAMI.1980.4767008
142. Jain AK, Duin RPW, Mao J (2000) Statistical pattern recognition: a review. IEEE Trans Pattern Anal Mach Intell 22(1):4–37. https://doi.org/10.1109/34.824819
143. Hosny A, Parmar C, Quackenbush J, Schwartz LH, Aerts HJWL (2018) Artificial intelligence in radiology. Nat Rev Cancer 18(8):500–510. https://doi.org/10.1038/s41568-018-0016-5
144. Ranjith G, Parvathy R, Vikas V, Chandrasekharan K, Nair S (2015) Machine learning methods for the classification of gliomas: initial results using features extracted from MR spectroscopy. Neuroradiol J 28(2):106–111. https://doi.org/10.1177/1971400915576637
145. Bacchi S et al (2019) Deep learning in the detection of high-grade glioma recurrence using multiple MRI sequences: a pilot study. J Clin Neurosci 70:11–13. https://doi.org/10.1016/j.jocn.2019.10.003
146. Ortega-Martorell S, Julià-Sapé M, Lisboa P, Arús C (2016) "Pattern recognition analysis of MR spectra" in eMagRes. John Wiley and Sons Ltd, Chichester, UK, pp 945–958
147. Menze BH, Wormit M, Bachert P, Lichy M, Schlemmer H-P, Hamprecht FA (2005) "Classification of In vivo magnetic resonance spectra" in classification — the ubiquitous challenge. Springer-Verlag, Berlin/Heidelberg, pp 362–369
148. Hagberg G (1998) From magnetic resonance spectroscopy to classification of tumors. A review of pattern recognition methods. NMR Biomed 11(4–5):148–156. https://doi.org/10.1002/(SICI)1099-1492(199806/08)11:4/5%3c148::AID-NBM511%3e3.0.CO;2-4
149. Howells SL, Maxwell RJ, Griffiths JR (1992) Classification of tumour 1H NMR spectra by pattern recognition. NMR Biomed 5(2):59–64. https://doi.org/10.1002/nbm.1940050203
150. García-Gómez JM et al (2009) Multiproject-multicenter evaluation of automatic brain tumor classification by magnetic resonance spectroscopy. MAGMA 22(1):5–18. https://doi.org/10.1007/s10334-008-0146-y
151. Somorjai RL et al (1996) Classification of 1H MR spectra of human brain neoplasms: the influence of preprocessing and computerized consensus diagnosis on classification accuracy. J Magn Reson Imaging 6(3):437–444. https://doi.org/10.1002/jmri.1880060305
152. Dikaios N (2021) Deep learning magnetic resonance spectroscopy fingerprints of brain tumours using quantum mechanically synthesised data. NMR Biomed 34(4):1–11. https://doi.org/10.1002/nbm.4479
153. Iqbal Z, Nguyen D, Hangel G, Motyka S, Bogner W, Jiang S (2019) Super-resolution 1H magnetic resonance spectroscopic imaging utilizing deep learning. Front Oncol 9(October):1–13. https://doi.org/10.3389/fonc.2019.01010
154. Ronneberger O, Fischer P, Brox T (2015) U-Net: Convolutional networks for biomedical image segmentation. Lect Notes Comput Sci (including Subser. Lect. Notes Artif. Intell. Lect. Notes Bioinformatics) 9351:234–241. https://doi.org/10.1007/978-3-319-24574-4_28
155. Di Ieva A, Choi C, Magnussen JS (2018) Spectrobiopsy in neurodiagnostics: the new era. Neuroradiology 60(2):129–131. https://doi.org/10.1007/s00234-017-1957-1
156. Sabatier J et al (1999) Characterization of choline compounds with in vitro 1H magnetic resonance spectroscopy for the discrimination of primary brain tumors. Invest Radiol 34(3):230–235. https://doi.org/10.1097/00004424-199903000-00013
157. Wilson M et al (2019) Methodological consensus on clinical proton MRS of the brain: review and recommendations. Magn Reson Med 82(2):527–550. https://doi.org/10.1002/mrm.27742
158. An L, Araneta MF, Victorino M, Shen J (2020) Signal enhancement of glutamine and glutathione by single-step spectral editing. J Magn Reson. https://doi.org/10.1016/J.JMR.2020.106756
159. Venneti S et al (2015) Glutamine-based PET imaging facilitates enhanced metabolic evaluation of gliomas in vivo. Sci Transl Med. https://doi.org/10.1126/SCITRANSLMED.AAA1009
160. Altman BJ, Stine ZE, Dang CV (2016) From Krebs to clinic: glutamine metabolism to cancer therapy. Nat Rev Cancer 16(10):619–634. https://doi.org/10.1038/nrc.2016.71
161. Choi YK, Park KG (2018) Targeting glutamine metabolism for cancer treatment. Biomol Ther (Seoul) 26(1):19–28. https://doi.org/10.4062/BIOMOLTHER.2017.178
162. Tiwari V et al (2020) In vivo MRS measurement of 2-hydroxyglutarate in patient-derived IDH-mutant xenograft mouse models versus glioma patients. Magn Reson Med 84(3):1152–1160. https://doi.org/10.1002/mrm.28183
163. Di Ieva A, Magnussen JS, McIntosh J, Mulcahy MJ, Pardey M, Choi C (2020) Magnetic resonance spectroscopic assessment of isocitrate dehydrogenase status in gliomas: the new frontiers of spectrobiopsy in neurodiagnostics. World Neurosurg 133:e421–e427. https://doi.org/10.1016/j.wneu.2019.09.040